doi:10.1093/plphys/kiab011 PLANT PHYSIOLOGY 2021: 185: 1943–1965

Plant Physiology

Research Article

Ubiquitylome analysis reveals a central role for the ubiquitin-proteasome system in plant innate immunity

Xiyu Ma,[1,†] Chao Zhang,[2,†] Do Young Kim,[3,4,†] Yanyan Huang,[1] Elizabeth Chatt,[5] Ping He ,[1] Richard D. Vierstra [3,5,‡] and Libo Shan [1,2,*,‡]

1 Department of Biochemistry and Biophysics, Texas A&M University, College Station, Texas 77843
2 Department of Plant Pathology and Microbiology, Texas A&M University, College Station, Texas 77843
3 Department of Genetics, University of Wisconsin–Madison, 425-G Henry Mall, Madison, Wisconsin 53706
4 Advanced Bio Convergence Center, Pohang Technopark, Gyeong-Buk 37668, South Korea
5 Department of Biology, Washington University in St. Louis, St. Louis, Missouri 63130

*Author for communication: lshan@tamu.edu
†These authors contributed equally.
‡Senior authors.

R.D.V., P.H., and L.S. conceived the project, designed the experiments, and analyzed the data. X.M., C.Z., D.Y.K., Y.H., and E.C. performed the experiments and analyzed the data. X.M., C.Z., R.D.V., and L.S. wrote the manuscript with inputs from all co-authors.

The author responsible for distribution of materials integral to the findings presented in this article in accordance with the policy described in the Instructions for Authors (https://academic.oup.com/plphys/pages/general-instructions) is: Libo Shan (lshan@tamu.edu).

Abstract

Protein ubiquitylation profoundly expands proteome functionality and diversifies cellular signaling processes, with recent studies providing ample evidence for its importance to plant immunity. To gain a proteome-wide appreciation of ubiquitylome dynamics during immune recognition, we employed a two-step affinity enrichment protocol based on a 6His-tagged ubiquitin (Ub) variant coupled with high sensitivity mass spectrometry to identify *Arabidopsis* proteins rapidly ubiquitylated upon plant perception of the microbe-associated molecular pattern (MAMP) peptide flg22. The catalog from 2-week-old seedlings treated for 30 min with flg22 contained 690 conjugates, 64 Ub footprints, and all seven types of Ub linkages, and included previously uncharacterized conjugates of immune components. In vivo ubiquitylation assays confirmed modification of several candidates upon immune elicitation, and revealed distinct modification patterns and dynamics for key immune components, including poly- and monoubiquitylation, as well as induced or reduced levels of ubiquitylation. Gene ontology and network analyses of the collection also uncovered rapid modification of the Ub-proteasome system itself, suggesting a critical auto-regulatory loop necessary for an effective MAMP-triggered immune response and subsequent disease resistance. Included targets were UBIQUITIN-CONJUGATING ENZYME 13 (UBC13) and proteasome component REGULATORY PARTICLE NON-ATPASE SUBUNIT 8b (RPN8b), whose subsequent biochemical and genetic analyses implied negative roles in immune elicitation. Collectively, our proteomic analyses further strengthened the connection between ubiquitylation and flg22-based immune signaling, identified components and pathways regulating plant immunity, and increased the database of ubiquitylated substrates in plants.

Received September 15, 2020. Accepted December 22, 2020. Advance access publication January 28, 2021
Published by Oxford University Press on behalf of American Society of Plant Biologists 2021. This work is written by US Government employees and is in the public domain in the US.

Downloaded from https://academic.oup.com/plphys/article/185/4/1943/6122724 by guest on 30 April 2021

Introduction

Post-translational modifications (PTMs), such as phosphorylation, methylation, acetylation, glycosylation, myristoylation, and ubiquitylation diversify protein behaviors, thus increasing the functionality and regulation of the proteome. As one of the most common PTMs, ubiquitylation is involved in nearly all physiological and signaling processes in plants, including hormone perception, photomorphogenesis, circadian rhythms, self-incompatibility, and defense against biotic and abiotic challenges (Vierstra, 2009; Trujillo and Shirasu, 2010; Guerra and Callis, 2012; Zhou and Zeng, 2017). Attachment of the 76-amino acid ubiquitin (Ub) moiety occurs most commonly to accessible lysines (K) within the target via an isopeptide bond that links to the carboxyl (C)-terminal glycine of Ub.

This conjugation is typically mediated through a stepwise enzymatic cascade consisting of a Ub-activating enzyme (UBA, or E1), a Ub-conjugating enzyme (UBC, or E2), and finally, a Ub-protein ligase (or E3), the latter of which has greatly expanded and diversified in plants to recognize a plethora of substrates. Additional Ubs can become attached to one or more of the seven lysine residues (K6, K11, K27, K29, K31, K48, and K63) or the amino (N)-terminal amide nitrogen within previously attached Ubs, resulting in a myriad of poly-Ub chain architectures that provide additional functional diversity (Vierstra, 2009; Komander and Rape, 2012). The most common internal linkage involves lysine 48 (K48), whose poly-Ub chains mainly target proteins for breakdown by the 26S proteasome, a multisubunit proteolytic complex that recognizes the Ub moieties (Vierstra, 2009; Zhou and Zeng, 2017). Although not as well understood in plants (Paez Valencia et al., 2016; Zhou and Zeng, 2017; Romero-Barrios and Vert, 2018), other types of poly-Ub linkages, involving K6, K11, K27, K29, K33, or K63, and monoubiquitylation in which only a single Ub is attached, have also been connected to many intracellular events, including protein trafficking, signal transduction, protein–protein interactions, and protein degradation through autophagy (Komander and Rape, 2012; Yin et al., 2020).

In recent years, a myriad of plant defenses against a range of pathogens has become apparent. The front line of defense is to block pathogen entry by erecting physical barriers, such as wax layers, cell walls, cuticular lipids, cutin, and callose, which can be strengthened during infection (Thordal-Christensen, 2003). As the first line of inducible defense, plants rely on innate immune responses to fend off infections internally, which are elicited upon recognition of pathogen- or microbe-associated molecular patterns (PAMPs/MAMPs) for pattern-triggered immunity (PTI), or pathogen-encoded effectors for effector-triggered immunity (ETI; Spoel and Dong, 2012; Zhou and Zhang, 2020). The host receptors known to detect these patterns/effectors are either receptor-like kinases (RLKs) or receptor-like proteins (RLPs; Böhm et al., 2014; Couto and Zipfel, 2016). The best understood is the RLK receptor FLAGELLIN SENSING 2 (FLS2) and its co-receptor BRASSINOSTEROID INSENSITIVE 1-ASSOCIATED KINASE 1 (BAK1) that recognizes the bacterial 22-amino-acid flagellin epitope flg22. Subsequently, PTI signaling is relayed through receptor-like cytoplasmic kinases (RLCKs), mitogen-activated protein kinase (MAPK) cascade, and transcription factors, which trigger diverse immune responses, including the production of reactive oxygen species (ROS) and the stress hormone ethylene (Couto and Zipfel, 2016; Yu et al., 2017). Pathogen effectors are recognized directly or indirectly by NUCLEOTIDE-BINDING SITE LEUCINE-RICH REPEAT (NBS-LRR) proteins (NLRs), which often leads to localized cell death at the infection sites known as the hypersensitive response (HR; Cui et al., 2015).

Protein ubiquitylation is also emerging as a dynamic process in both PTI and ETI signaling (Cheng and Li, 2012; Zhou and Zeng, 2017; Adams and Spoel, 2018). As examples, the MAMP receptor FLS2 is ubiquitylated upon ligand engagement by the E3s PLANT U-BOX 12 (PUB12) and PUB13, resulting in FLS2 degradation (Lu et al., 2011; Zhou et al., 2015), whereas PUB13 also directs the ubiquitylation and degradation of LYSIN MOTIF RECEPTOR KINASE 5 (LYK5), an RLK that recognizes the fungal cell wall polysaccharide chitin (Liao et al., 2017). The RLCK *BOTRYTIS*-INDUCED KINASE 1 (BIK1), which provides a convergent signaling hub downstream of multiple MAMP receptors, is strongly regulated by Ub addition (Wang et al., 2018; Ma et al., 2020). Two U-box E3s, PUB25, and PUB26 polyubiquitylate BIK1 to control its steady-state levels, whereas the RING-type E3 ligases, RING-H2 FINGER A3A (RHA3A) and RHA3B, monoubiquitylate BIK1 to direct its endocytosis and signaling activation (Wang et al., 2018; Ma et al., 2020). Additionally, the PUB22, PUB23, and PUB24 E3s work collectively to negatively regulate PTI responses through modification of EXOCYST SUBUNIT EXO-70 FAMILY PROTEIN B2 (EXO70B2), which promotes vesicle trafficking (Stegmann et al., 2012). Levels of several NLR proteins, including RESISTANT TO *PSEUDOMONAS SYRINGAE* 2 (RPS2) and SUPPRESSOR OF *npr1-1* CONSTITUTIVE 1 (SNC1), are also regulated by CONSTITUTIVE EXPRESSOR OF PR GENES 1 (CPR1), which is the target-recognition F-Box subunit within an SKP1-CULLIN1-F-BOX (SCF) E3 complex (Cheng et al., 2011; Gou et al., 2012). Despite these examples, a systematic investigation of ubiquitylation during plant immune activation is currently lacking.

Recent advances in proteomics have enabled high-throughput and comprehensive views of ubiquitylomes under specific physiological conditions. The first catalog was generated with yeast in which wild-type Ub was replaced by a 6His-tagged variant to enable enrichment of ubiquitylated proteins by nickel-nitrotrilotriacetic acid (Ni-NTA) affinity chromatography under denaturing conditions, followed by liquid chromatography–mass spectrometric (LC–MS) analysis of the trypsinized preparations (Peng et al., 2003). Saracco et al. (2009) then adopted this strategy for plants through the creation of a transgenic *Arabidopsis* line that constitutively expresses a hexa-6His-Ub concatamer, which is post-translationally processed into functional 6His-Ub

Downloaded from https://academic.oup.com/plphys/article/185/4/1943/6122724 by guest on 30 April 2021

monomers. Subsequently, Ub-binding domains were exploited for the additional enrichment needed for more complex proteomes (Maor et al., 2007). Further improvements included Tandem-repeated Ub-binding entities (TUBEs), in which natural Ub-binding domains were oligomerized to increase enrichment and yield (Hjerpe et al., 2009). By combining TUBEs with the Ni-NTA affinity chromatography, stringent purifications were possible, which enabled the confident detection of more than 900 ubiquitylated proteins in *Arabidopsis* (Kim et al., 2013; Aguilar-Hernandez et al., 2017). Notably, a number of Ub targets associated with disease resistance were identified.

Here, we employed this improved two-step TUBEs purification approach coupled with deep MS analysis of *Arabidopsis* seedlings before and shortly after exposure to flg22. The resulting ubiquitylome catalog revealed extensive proteome-wide changes soon after MAMP perception and uncovered a large number of ubiquitylated candidates potentially connected to plant innate immunity. We further observed by in vivo ubiquitylation assays distinct ubiquitylation patterns and dynamics for several immunity components, including key regulators that were modified by multiple ubiquitylation events. Interestingly, several Ub-proteasome pathway components were also confirmed as Ub targets upon PTI immune elicitation, including the E2 UBC13 and proteasome subunit REGULATORY PARTICLE NON-ATPASE SUBUNIT 8b (RPN8b). Taken together, our study identified connections between the Ub-proteasome system (UPS) and pathogen immunity as well as provided a valuable resource to further study this PTM during immune activation.

Results

TUBEs enrichment of ubiquitylated *Arabidopsis* proteins upon flg22 treatment

To gain a global perspective of ubiquitylation during PTI elicitation, we employed a two-step TUBEs purification protocol to enrich for ubiquitylated proteins soon after exposure of 2-week-old *A. thaliana* ecotype Col-0 seedlings to flg22 (Kim et al., 2013), which was based on a transgenic line harboring a synthetic *UBQ* gene encoding six 6His-Ub repeats expressed under the control of the Cauliflower mosaic virus (CaMV) 35S promoter (Saracco et al., 2009). The polymer is processed by endogenous deubiquitylases (DUBs) to release tagged and fully functional Ub monomers (Isono and Nagel, 2014). In the first step, extracts from *hexa-6His-UBQ* seedlings either untreated or treated for 30 min to flg22 were prepared in a non-denaturing buffer containing the non-ionic detergent Triton X-100 and a protease inhibitor cocktail to minimize DUB activities that would disassemble Ub conjugates post homogenization, and then enriched for Ub-bearing species by TUBEs chromatography (Raasi et al., 2004; Hjerpe et al., 2009), using as the ligand four copies of the Ub-associated domain (UBA) sequence from human hHR23A interconnected through a short flexible linker, and fused with GLUTATHIONE S-TRANSFERASE (GST; Figure 1, A). Previous studies show that this GST-4X(UBA) fusion binds effectively to native Ub-conjugates bearing various chain topologies from *Arabidopsis*, thus allowing us to interrogate its near complete ubiquitylome (Kim et al., 2013; Aguilar-Hernandez et al., 2017). In the second step, we enriched for poly-His-containing proteins via Ni-NTA chromatography under strong denaturing conditions using buffers containing 7 M guanidine-HCl and 8 M urea for the application and washing steps, respectively, followed by elution with a buffer containing 8 M urea and 400 mM imidazole (Figure 1, B).

As seen in Figure 1, C and D, eluants from the TUBEs and Ni-NTA columns prepared with control and flg22-treated *hexa-6His-UBQ* seedlings had substantially more ubiquitylated species than those obtained from wild-type seedlings, as detected by immunoblot analysis with rabbit anti-Ub antibodies. They appeared particularly enriched in high molecular-mass Ub conjugates, with limited amounts of free Ub or the Ub dimer that were easily seen in total seedling extracts (Figure 1, D). The main contaminant was RIBULOSE-1,5-BISPHOSPHATE CARBOXYLASE/OXYGENASE (Rubisco), which is often recognized by antibodies generated in rabbits.

Identification of Ub-conjugates by LC–MS/MS

Ub-conjugates from the *hexa-6HIS-UBQ* plants were trypsinized, separated by reversed-phase nanoflow LC, and subjected to tandem MS (MS/MS) using a Velos LTQ mass spectrometer in the high-energy collision mode (Figure 1, B). Peptides were matched to the *Arabidopsis* ecotype Col-0 protein database (IPI database, version 3.85; http://www.arabidopsis.org) using SEQUEST, based on the identification of two or more different matching peptides with a $\leqslant$1% false discovery rate (FDR), or if a single matching peptide of equivalent stringency was identified that harbored a canonical Ub footprint (Kim et al., 2013). This footprint was detected by the presence of a di-Gly remnant (Gly–Gly) from Ub isopeptide linked to a lysine within the peptide, which increased the monoisotopic mass of the residue by 114 Da as well as protected the site from trypsin cleavage (Peng et al., 2003; Saracco et al., 2009). To help eliminate contaminants that bind non-specifically to the TUBEs and/or Ni-NTA columns, a background LC–MS/MS database was also generated with wild-type plants that underwent the same two-step affinity protocol; these proteins were subtracted from the *hexa-6HIS-UBQ* datasets to obtain the final ubiquitylome catalog (Kim et al., 2013). In total, we generated MS/MS datasets from three biological replicates for control, untreated, and flg22-treated seedlings for final comparisons.

The summation of this MS analysis enabled the detection of 391 Ub conjugates in control samples (204, 210, and 250 proteins for biological replicates 1, 2, and 3, respectively) and 570 Ub conjugates in the flg22-treated samples (391, 400, and 142 proteins for biological replicates 1, 2, and 3, respectively; Supplemental Table S1). Notably, 90 proteins in the control samples and 88 proteins in the flg22-treated

Downloaded from https://academic.oup.com/plphys/article/185/4/1943/6122724 by guest on 30 April 2021

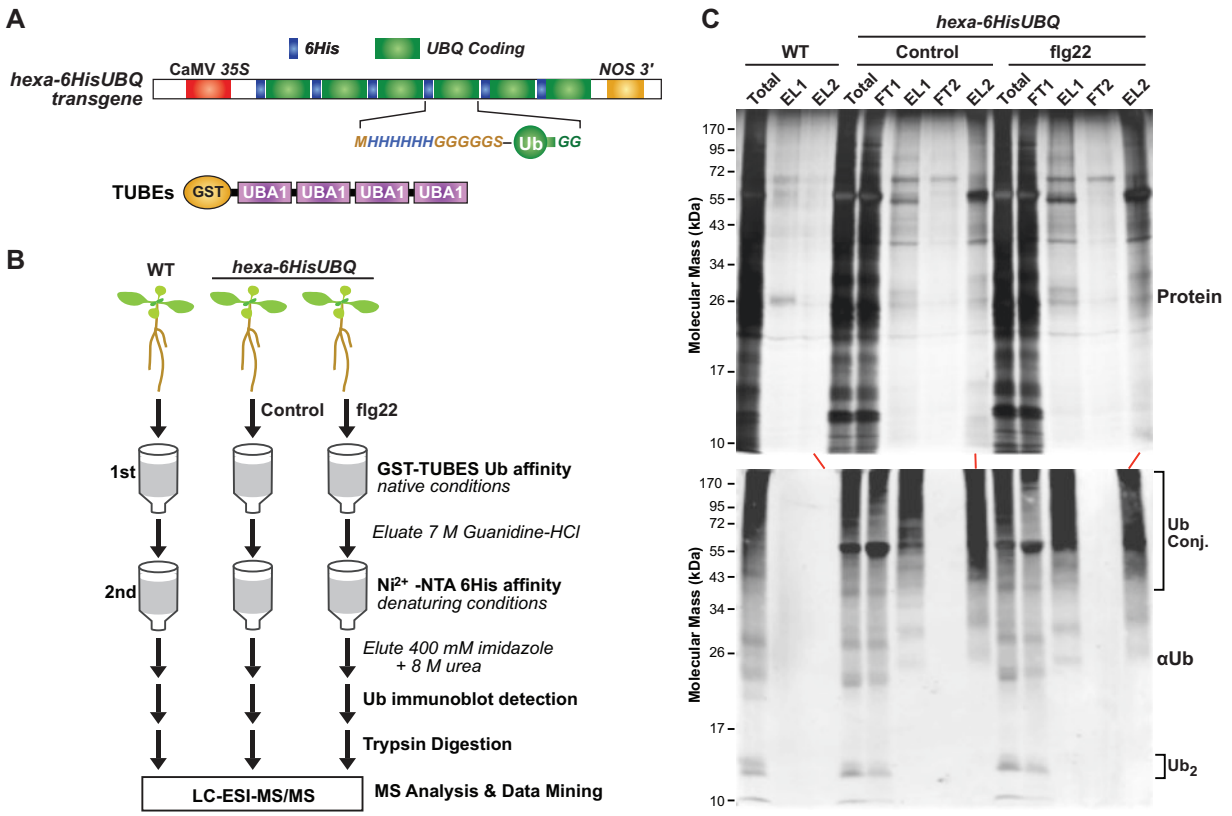

Figure 1 Two-step affinity purification of ubiquitylated proteins from transgenic *Arabidopsis* expressing *6HIS-UBQ* treated with or without flg22. A, Diagram of the *p35S:hexa-6HIS-UBQ* transgene. A synthetic *UBQ* gene encoding six repeats of a Ub monomer N-terminally tagged with a 6His sequence followed by a glycine (G)-rich linker (MHHHHHHGGGGGSA) was fused head-to-tail to form a single in-frame *hexa-6His-UBQ* transgene expressed under the control of the constitutive CaMV *35S* promoter (Saracco et al., 2009). B, Flow chart describing the proteomic approach to stringently identify Ub conjugates from *Arabidopsis p35S:hexa-6HIS-UBQ* seedlings. Ubiquitylated proteins were first enriched by the UBA-Ub affinity using GST-TUBEs beads under the native condition followed by Ni-NTA chromatography under the denaturing condition. The eluants were digested with trypsin and subjected to LC/ESI–MS/MS analysis. C, Ubiquitylated proteins isolated from *Arabidopsis* plants expressing 6His-Ub by the two-step affinity purification. Ubiquitylated proteins enriched as outlined in (B) were subjected to SDS–PAGE and by either stained for protein with silver (top) or immunoblotted with anti-Ub antibodies (bottom). Samples from wild-type seedlings (WT) incubated with both GST-TUBEs and Ni-NTA beads were included for comparison. FT and EL represent the flow-through and eluted fractions, respectively, from the TUBEs affinity (1) and Ni-NTA affinity columns (2). The total represents the total protein extracts before affinity purifications. The migration positions of the Ub dimers (Ub_2), and Ub conjugates (Ub-conj) are indicated by the brackets.

samples were consistently identified in all three biological replicates, which likely represented a high abundance of ubiquitylated species. When combined, we uncovered 690 ubiquitylated proteins with high confidence; 419 were confined to either control or flg22-treated samples, whereas 271 proteins were present in both (Figure 2, A). We detected 299 proteins unique to the flg22-treated samples versus 120 proteins unique to the control samples, implying that the PTI elicitation rapidly and markedly increases ubiquitylation in Arabidopsis (Figure 2, A).

Gene ontology analyses of flg22-treated and -untreated ubiquitylomes

To gain a global perspective for how ubiquitylation is influenced by immune elicitation, we classified the identified targets in the control and flg22-treated ubiquitylomes based on their known or predicted functions within the Gene Ontology (GO) database using the DAVID Functional Annotation Tool (Huang da et al., 2009). As shown in Figure 2, B, the numbers of significantly enriched genes (FDR <0.05) in flg22-treated ubiquitylome were larger than those in the control for the three main GO domains ("Biological Processes": 104 versus 82, "Molecular Functions": 59 versus 45, and "Cellular Components" 74 versus 62). Enrichments included the GO terms "defense response to fungus," and "innate immune response," which were found only in the flg22-treated ubiquitylome, whereas the related terms "defense response to bacterium," "regulation of stomatal movement," "defense response by callose deposition," and "oxidation–reduction process" were more significantly enriched (Figure 2, B and C).

When compared with the total proteome, we also saw significant enrichment for GO terms associated with "Ub-dependent protein catabolic process" (Biological process), and "Cul4-RING E3 Ub ligase" (Cellular components) in both control and flg22-treated ubiquitylomes, as were the GO

Downloaded from https://academic.oup.com/plphys/article/185/4/1943/6122724 by guest on 30 April 2021

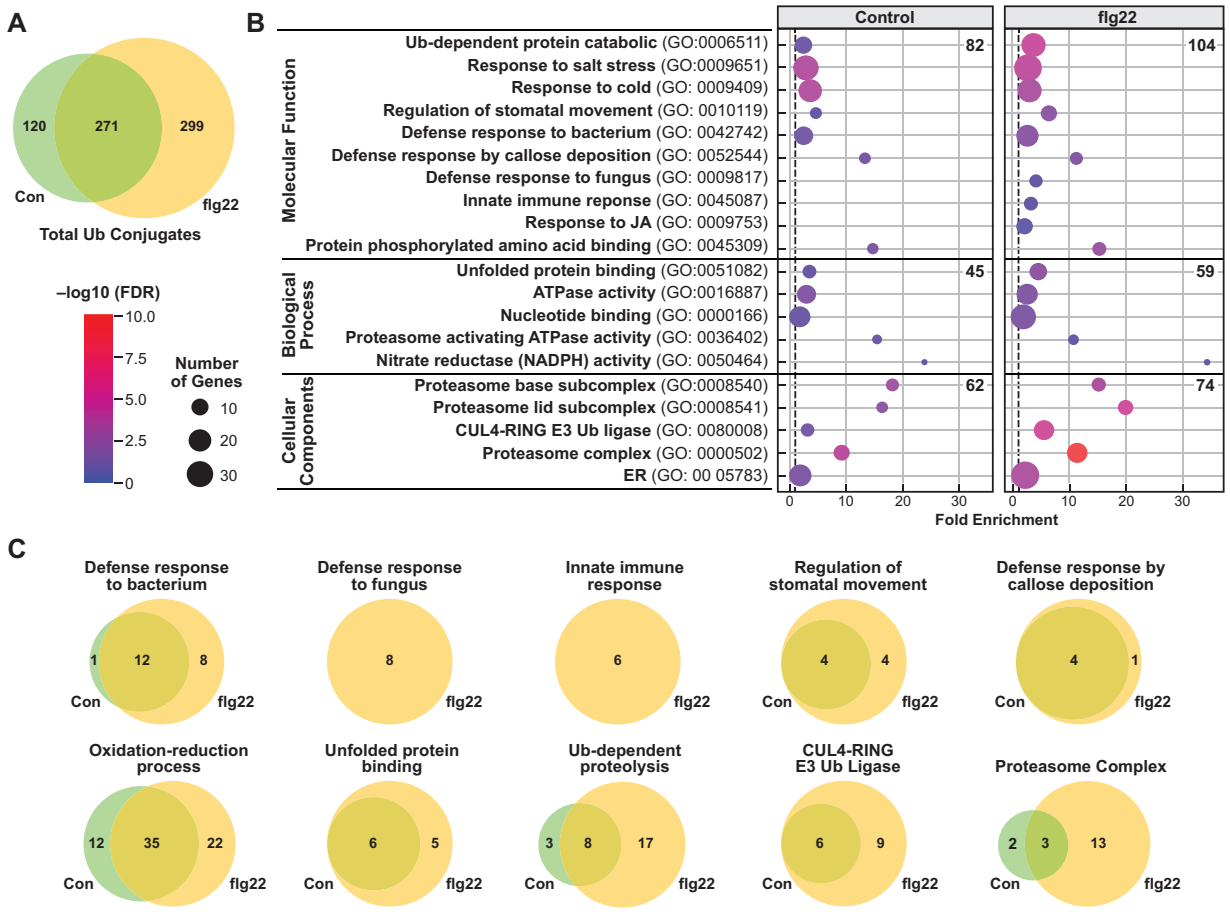

Figure 2 GO analysis of flg22-treated and -untreated ubiquitylomes. A, Venn diagram showing the overlap of the total ubiquitylated proteins isolated from plants with or without flg22 exposure. B, GO enrichment of ubiquitylated proteins in control or flg22-induced ubiquitylomes. GO analysis in biological processes, molecular functions, and cellular components was performed using the DAVID Functional Annotation Tool (Huang da et al., 2009) and GO annotations from the TAIR GO database (http://www.arabidopsis.org/). The fold enrichment was calculated based on the frequency of proteins annotated to the term compared with their frequency in the total proteome. The dot size indicates the number of genes associated with each process and the dot color indicates the significance of the enrichment. FDR was based on the corrected *P*-values. The vertical gray dashed line represents a fold enrichment of 1. The total number of GO terms was listed under each GO domain (biological processes, molecular functions, and cellular components). The selected terms related to stress and the UPS are shown. C, Venn diagram showing the overlaps of ubiquitylated proteins with or without flg22 in the selected categories. Proteins were categorized into functional groups based on the GO annotations; those related to defense responses and the UPs are shown.

terms related to stress, such as "response to salt stress" and "response to cold stress" (Figure 2, B). Strikingly, this enrichment in Ub-related events was more robust in the flg22-treated versus control ubiquitylomes (3.7-fold versus 2.4-fold for "ubiquitin-dependent protein catabolic process" and 5.5-fold versus 3.2-fold for "Cul4-RING E3 Ub ligase," respectively). A prevalence for UPS components in the flg22-treated samples was also evident for proteins associated with "proteasomes" (11.4-fold versus 9.2-fold, respectively; Figure 2, C). Taken together, this non-targeted MS analysis directly connected rapid flg22-induced ubiquitylation to Arabidopsis proteins associated with immunity and the UPS itself.

Global ubiquitylation of immunity-related proteins

Among the identified Ub conjugates were many key immunity-related proteins (Table 1). To link these ubiquitylated species to immune signaling globally, we generated an interaction network using the Search Tool for Retrieval of Interacting Genes/Proteins (STRING) database (Szklarczyk et al., 2015), which revealed an interconnected web with defense-related proteins often situated at key hubs (Figure 3, A and B). Examples included plasma membrane-resident, leucine-rich repeat-RLKs (LRR-RLKs), such as RECEPTOR-LIKE KINASE 7 (RLK7) and SUPPRESSOR OF *BIR1-1*/EVERSHED (SOBIR1/EVR) that interact with multiple LRR-RLP receptors (Figure 3, A and B). Whereas SOBIR1 serves as a common component in RLP-mediated plant immunity (Liebrand et al., 2014; Albert et al., 2015), RLK7 is a receptor for PAMP-INDUCED PEPTIDE 1 (PIP1), which acts as a damage-associated molecular pattern (DAMP) to amplify plant immune signaling (Hou et al., 2014). Additionally, LysM RLK1-INTERACTING KINASE 1 (LIK1), which was specific to the flg22-treated ubiquitylome,

Downloaded from https://academic.oup.com/plphys/article/185/4/1943/6122724 by guest on 30 April 2021

Table 1 Ubiquitylation of immunity-related proteins identified from *6HIS-UBQ* seedlings treated with or without flg22

Locus ID	Other names	Description	Category	Role in immunity	Condition	References
AT4G34230	CAD5	Cinnamyl alcohol dehydrogenase 5	Preformed defense	Involves in lignin biosynthesis and disease resistance against *Pst* DC3000.	flg22	Tronchet et al. (2010)
AT3G10340	PAL4	Phenylalanine ammonia-lyase 4	Preformed defense	Functions in the lignin and SA pathway in plant disease resistance.	flg22	Huang et al. (2010) and Chen et al. (2017)
AT5G36890	BGLU42	Beta glucosidase 42	Preformed defense	Promotes disease resistance against *B. cinerea*, *H. arabidopsidis*, and *Pst* DC3000	flg22	Zamioudis et al. (2014) and Stringlis et al. (2018)
AT3G53420	PIP2A, PIP2;1	Plasma membrane intrinsic protein 2A	Preformed defense	Involves in stomatal closure triggered by abscisic acid (ABA) or flg22 for water and H_2O_2 transport activities	flg22	Rodrigues et al. (2017)
AT1G09970	RLK7	Leucine-rich repeat receptor-like kinase 7	RLK	Receptor for PIP1 defense peptide in PTI signaling	flg22	Pitorre et al. (2010) and Hou et al. (2014)
AT3G14840	LIK1	LysM RLK1-interacting kinase 1	RLK	Interacts with CERK1 and positively regulates resistance to necrotrophic pathogens.	flg22	Le et al. (2014)
AT1G48480	RKL1	Receptor-like protein kinase 1	RLK	Characterized in this study	flg22	Tarutani et al. (2004)
AT2G31880	SOBIR1, EVR	Leucine-rich repeat receptor-like protein	RLK	Interacts with multiple LRR–RLP and functions as a common component in RLP-mediated plant immunity	flg22	Liebrand et al. (2014) and Albert et al. (2015)
AT1G53350	RPP8L2	RPP8-like protein 2; Resistance protein; CC-NBS-LRR	CNL	Belongs to CNL-D subclass, may involve in controlling virus infection	flg22	Revers et al. (2003); Bakker et al. (2006); Tan et al. (2007); Mondragon-Palomino et al. (2017)
AT5G45240		Resistance protein; TIR-NBS-LRR	TNL	Uncharacterized	flg22	
AT5G48770		Resistance protein; TIR-NBS-LRR	TNL	Uncharacterized	flg22	
AT5G13530	KEG	RING E3 Ub-protein ligase; KEEP ON GOING	Signaling	Essential for the secretion of apoplast antimicrobial proteins	flg22	Gu and Innes (2011)
AT2G46240	BAG6	BCL-2-associated athanogene 6	Signaling	Co-chaperone regulating diverse cellular pathways, such as programmed cell death, abiotic stress responses, and plant basal resistance	flg22	Li et al. (2016)
AT2G21660	CCR2, GRP7	Cold, circadian rhythm, and RNA binding 2; glycine-rich RNA-binding protein 7	Signaling	Associates with FLS2 mRNA and proteins; maintains the FLS2 protein level	flg22	Nicaise et al. (2013)
AT4G34460	AGB1, ELK4	Heterotrimeric G-protein beta-subunit; ERECTA-LIKE 4	Signaling	Complexes with FLS2 and regulates BIK1 stability	flg22	Liu et al. (2013) and Liang et al. (2016)
AT5G03520	RAB8C, RABE1D	Rab GTPase homolog 8C	Signaling	Involves in protein trafficking, interacts with AvrPto, and accumulates in response to bacterial infection	flg22	Speth et al. (2009) and Hou and Gao (2017)
AT3G21220	MEK5, MKK5	MAPK kinase 5	Signaling	Activate MPK3 and MPK6 in PTI signaling.	flg22	Meng and Zhang (2013)
AT3G45640	MPK3	MAPK 3	Signaling	Activated by MAMP treatment in PTI signaling	flg22	Asai et al. (2002); Pecher et al. (2014); and Su et al. (2018)

(continued)

Downloaded from https://academic.oup.com/plphys/article/185/4/1943/6122724 by guest on 30 April 2021

Table 1 Continued

Locus ID	Other names	Description	Category	Role in immunity	Condition	References
AT2G33340	MAC3B; PUB60	MOS4-associated complex 3B; Plant U-Box 60 E3 ligase	Signaling	Localizes to the nucleus and involves in plant innate immunity	flg22	Monaghan et al. (2009)
AT1G77740	PIP5K2	Phosphatidylinositol-4-phosphate 5-kinase	Signaling	Responsible for PI(4,5)P2 biosynthesis; inhibits fungal pathogen development and triggers disease resistance	Control	Qin et al. (2020)
AT3G18130	RACK1C	Receptor for activated C kinase 1C	Signaling	Scaffold proteins connecting heterotrimeric G proteins with a MAPK cascade in plant immunity	Control, flg22	Nakashima et al. (2008); Cheng et al. (2015); and Su et al. (2015)
AT3G48090	EDS1	Enhanced disease susceptibility 1; a lipase-like protein	Signaling	Required for multiple TNL-mediated resistance.	flg22	Parker et al. (1996); Heidrich et al. (2011); and Cui et al. (2015)
AT3G50480	HR4	Homolog of RPW8	Signaling	Involved in autoimmunity mediated by RPP7 oligomerization	flg22	Li et al. (2020)
AT1G64790	ILA	ILITYHIA; HEAT repeat protein	SAR	Involved in immunity against bacterial infection, non-host resistance, and systemic acquired resistance	flg22	Monaghan and Li (2010)
AT2G44490	BGLU26, PEN2	Beta-glucosidase 26, PENETRATION 2	Preformed defense	Required for callose deposition and glucosinolate activation in pathogen-induced resistance	Control, flg22	Clay et al. (2009) and Pastorczyk and Bednarek (2016)
AT3G19450	CAD4	Cinnamyl alcohol dehydrogenase 4	Preformed defense	Involved in lignin biosynthesis and disease resistance to bacterial pathogens.	Control, flg22	Kim et al. (2004) and Tronchet et al. (2010)
AT4G03550	GSL5, PMR4	Callose synthase	Preformed defense	Required for callose formation induced by pathogen infections.	Control, flg22	Jacobs et al. (2003) and Wawrzynska et al. (2010)
AT1G63350		Resistance protein; CC-NBS-LRR	CNL	Uncharacterized	Control, flg22	
AT1G01560	MPK11	MAP Kinase 11	Signaling	Activated upon flg22 treatment	Control, flg22	Bethke et al. (2012) and Eschen-Lippold et al. (2012)
AT4G23650	CPK3	Calcium-dependent protein kinase 3	Signaling	Required for sphingolipid-induced cell death and viral infection	Control, flg22	Lachaud et al. (2013) and Perraki et al. (2017)
AT1G48630	RACK1B	Receptor for activated C kinase 1B	Signaling	Scaffold proteins connecting heterotrimeric G proteins with a MAPK cascade in plant immunity	Control, flg22	Nakashima et al. (2008); Cheng et al. (2015); and Su et al. (2015)

has been shown to interact with the fungal chitin receptor complex component CERK1 to positively regulate resistance against necrotrophic pathogens (Le et al., 2014). The LRR III protein RECEPTOR-LIKE KINASE 1 (RKL1), identified here as a flg22-triggered ubiquitylation substrate, was previously shown to modulate the activity of the aquaporin PLASMA MEMBRANE INTRINSIC PROTEIN (PIP) family during osmotic and oxidative stress together with its close homolog RLK902 (Bellati et al., 2016). Intriguingly, whereas RKL1 was not yet connected to pathogen defense, RLK902 had been shown to transmit an immune signal by phosphorylating the RLCK BRASSINOSTEROID-SIGNALING KINASE 1 (BSK1; Zhao et al., 2019).

Downstream of the immune receptor complexes are sequential phosphorylation events involving MAPK cascades driven by MAPK KINASE KINASES (MAPKK/MEKK), MAPK KINASES (MAPKK/MKK), and MAPKS (MPK) components (Meng and Zhang, 2013). Notably, MKK5, MPK3, and MPK11, which are known to become phosphorylated upon flg22 perception (Bethke et al., 2012), were detected here, with MKK5 and MPK3 only identified in the flg22-treated ubiquitylome (Figure 3, B). Heterotrimeric G-proteins, consisting of Gα, Gβ, and Gγ subunits, act as molecular switches to mediate diverse signal transduction events (Urano et al., 2013). In particular, *ARABIDOPSIS* G PROTEIN β-SUBUNIT1 (AGB1), which associates with FLS2 and regulates BIK1 stability during plant PTI (Liu et al., 2013; Liang et al., 2016), was identified in the flg22-treated samples. Ubiquitylated forms of RECEPTOR FOR ACTIVATED C KINASE (RACK)-1B and RACK1C, which scaffolds and

Downloaded from https://academic.oup.com/plphys/article/185/4/1943/6122724 by guest on 30 April 2021

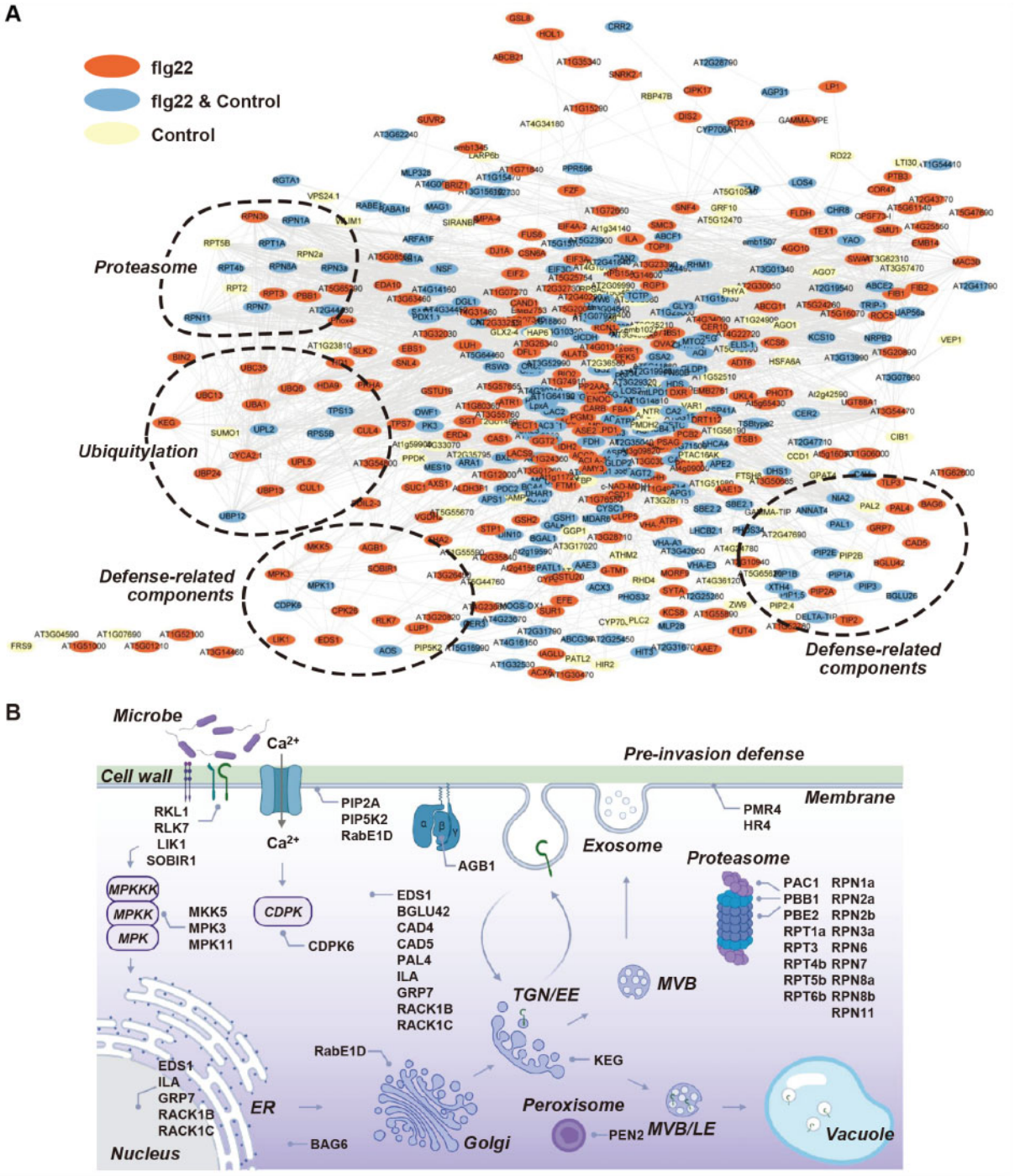

Figure 3 Protein interaction network of ubiquitylated proteins identified from *hexa-6HIS-UBQ* seedlings treated with or without flg22. A, Protein interaction networks were generated with the list of 391 (control) and 570 (flg22-treated) ubiquitylated proteins using the STRING database and visualized in Cytoscape. The node colors indicate proteins identified in control (yellow), flg22-treated (red), or both conditions (blue) of datasets. Clusters of the proteasome, ubiquitylation, and defense-related components are marked by dashed lines. B, Map of proposed subcellular locations and functions of immunity-related proteins identified in the ubiquitylome datasets.

connects heterotrimeric G proteins with MAPK cascades to form a unique signaling pathway in plant immunity (Cheng et al., 2015), were identified in both control and flg22-treated ubiquitylomes, or only the flg22-treated ubiquitylome, respectively.

Protein trafficking, regulated by a cascade of factors such as small GTPases from Rab subfamilies, also plays important roles in plant immunity (Gu et al., 2017). RabE1D, identified here in the flg22-treated ubiquitylome, is associated with Golgi and the plasma membrane and might regulate the

Downloaded from https://academic.oup.com/plphys/article/185/4/1943/6122724 by guest on 30 April 2021

apoplast secretion of anti-microbial proteins, such as PATHOGENESIS-RELATED PROTEIN 1 (PR1), that induce resistance against *Pseudomonas syringae* pv. *tomato* (*Pst*) DC3000 (Speth et al., 2009). Likewise, the E3 KEEP ON GOING (KEG), which localizes to the trans-Golgi network/early endosome (TGN/EE) compartments and is essential for TGN/EE-mediated secretion of PR1 and papain-like Cys protease C14 (Gu and Innes, 2011), appears to be ubiquitylated by a flg22-induced event (Figure 3, B).

ETI components were also identified as flg22-specific ubiquitylation substrates. Included were four uncharacterized NLR proteins (AT1G53350, AT1G63350, AT5G45240, and AT5G48770) along with ENHANCED DISEASE SUSCEPTIBILITY 1 (EDS1), which is a nucleocytoplasmic lipase-like protein indispensable for both basal immunity and multiple TOLL-INTERLEUKIN 1 RECEPTOR (TIR) domain NLR-mediated resistance events (Cui et al., 2015; Lapin et al., 2020). Proteins implicated in long-distance resistance were identified in the flg22-treated ubiquitylome, such as the HEAT-repeat protein ILITHYIA (ILA) that encourages systemic acquired resistance (Monaghan and Li, 2010). The peroxisome-localized glycol hydrolase PENETRATION2 (PEN2) was seen in all control and flg22-treated samples and thus considered to be a high abundance Ub target. PEN2, together with PEN1 and PEN3, actuate a cell wall-based defense against non-adapted pathogens by limiting pathogen entry (Figure 3, B; Collins et al., 2003; Clay et al., 2009; Fuchs et al., 2016). Similarly, the lignin biosynthetic enzymes, namely CINNAMYL ALCOHOL DEHYDROGENASE 4 (CAD4), identified in both control and flg22-treated ubiquitylomes, and CAD5 identified only in flg22-treated ubiquitylomes, likely protect against pathogen invasion by modifying the lignin content of cell walls (Tronchet et al., 2010). The callose synthase POWDERY MILDEW RESISTANT 4 (PMR4), which is required for wound- and/or pathogen-induced callose formation (Meyer et al., 2009; Wawrzynska et al., 2010), was also found in both datasets (Figure 3, B). Taken together, our ubiquitylome profiles implicate Ub addition in multiple defense responses ranging from the preformed cell wall-based protection, to inducible PTI and ETI, and systemic defense (Figure 3, B).

Distinct ubiquitylation patterns and dynamics of immunity-related proteins upon flg22 elicitation

To examine more closely the ubiquitylation dynamics (+/− flg22) of several immunity-related substrates, we exploited a previously established in vivo ubiquitylation system in which FLAG-tagged Ub (FLAG-Ub) is co-expressed with HA- or Myc-tagged targets in wild-type Arabidopsis leaf protoplasts (ZHou et al., 2014). Ubiquitylated proteins are enriched by immunoprecipitation (IP) with anti-FLAG antibody beads and then probed by immunoblot analysis with anti-HA or anti-Myc antibodies to assay for possible ubiquitylated species.

As shown in Figure 4, A, we successfully confirmed the ubiquitylation of MPK3, MKK5, SOBIR1, and EDS1 using this in vivo system combined with HA- or Myc-tagged versions. For MPK3-HA, multiple ubiquitylated species were evident in anti-FLAG immunoprecipitates with a dominant form seen at ∼52 kDa. Being ∼8 kDa bigger than that of unmodified MPK3-HA (∼43.8 kDa), we consider it likely that it represents a monoubiquitylated form. Notably, ubiquitylation of MPK3-HA was transiently enhanced soon after flg22 treatment (10 min) but quickly returned to a basal level of modification at 30 min (Figure 4, A), even though the levels of unmodified MPK3-HA remained steady for up to 1 h of flg22 treatment (Figure 4, A), suggesting that MPK3 ubiquitylation triggered by flg22 helps relay the flg22 signal. By contrast, modification of MKK5-Myc, easily seen by a strong monoubiquitylated species, appeared to be constitutive, i.e. its level was unchanged by flg22 elicitation (Figure 4, B). For both SOBIR1-HA and EDS1-HA, poly-ubiquitylated species accumulated in the in vivo system. The smear of high molecular mass conjugates for SOBIR1 was strongly enhanced upon flg22 treatment (Figure 4, C). By contrast, the smear of high molecular-mass conjugates for EDS1 was largely reduced upon flg22 treatment (Figure 4, D). RKL1-HA was found constitutively poly-ubiquitylated in vivo, even though ubiquitylated RKL1 was only identified in flg22-treated seedlings in the proteomic analysis described earlier (Figure 4, E). Taken together, we confirmed the ubiquitylation of candidate proteins using this cell-based assay, which revealed surprisingly distinct ubiquitylation patterns and dynamics for the candidates upon immune elicitation with flg22.

Ubiquitylation of UPS components

As revealed above (Table 2 and Figures 2 and 3), multiple UPS components were preferentially identified in flg22-treated ubiquitylome. Included were the E1 UBA1, the E2 isoforms UBC13, and UBC35 (UBC13A), the E3 components CULLIN 1 (CUL1), CUL4, and UB-PROTEIN LIGASE 5 (UPL5), components of the 26S proteasome, and the DUBs Ub-Specific Proteases (UBP)-13 and UBP24, and a predicted Ub-Carboxy-Terminal Hydrolase (UCH; AT4G24320) expected to release free Ub monomers from poly-Ub chains and poly-Ub translation products. UPL5 is part of the single polypeptide HECT E3 family. By contrast, CUL1, together with S-PHASE KINASE-ASSOCIATED PROTEIN 1 (SKP1), RING BOX 1 (RBX1), and one of possibly >700 F-box protein variants, assemble into SCF-type E3 complexes (Hua and Vierstra, 2011), whereas the CUL4 scaffolds DNA DAMAGE-BINDING (DDB)-type E3 complexes assemble with RBX1, and one of over 85 DWD box-containing DDB proteins (Hua and Vierstra, 2011). Previously, DDB1 was implicated in *PR* gene expression and resistance to *Agrobacterium tumefaciens* infection in tomato (*Solanum lycopersicum*; Liu et al., 2012), which might explain the connection between CUL4 and immune elicitation, whereas UPL5 is required for SA- and NONEXPRESSER OF *PR* GENES 1 (NPR1)-mediated plant

Downloaded from https://academic.oup.com/plphys/article/185/4/1943/6122724 by guest on 30 April 2021

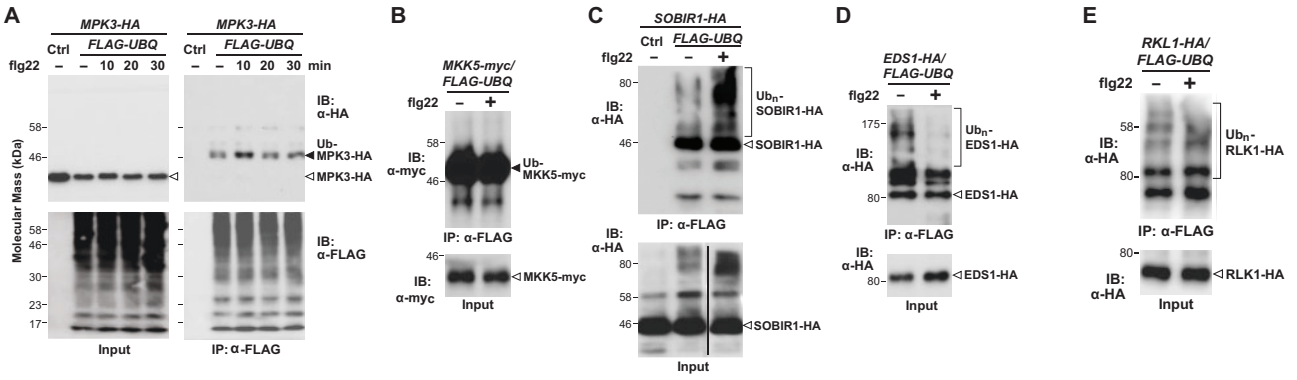

Figure 4 In vivo confirmation that several candidates are ubiquitylated in *Arabidopsis*. *Arabidopsis* wild-type protoplasts were co-transfected with FLAG-tagged Ub (*FLAG-UBQ*) and HA- or Myc-tagged substrate or a control vector (Ctrl) and incubated for 10 h followed by treatment with 100 nM flg22 for the indicated. Protein extracts were immunoprecipitated with anti-FLAG agarose beads (IP: α-FLAG) and the ubiquitylated proteins were immunoblotted with anti-HA or anti-Myc antibodies or anti-FLAG antibodies. The input controls were shown by an anti-HA/Myc or anti-FLAG immunoblots. A, Monoubiquitylation of MPK3 is enhanced upon flg22 treatment. Protoplasts were isolated at 0–30 min after flg22 exposure. B, Monoubiquitylation of MKK5 in vivo upon a 30-min treatment with flg22. C–E, SOBIR1, EDS1, and RKL1 were polyubiquitylated in vivo following a 30-min treatment with flg22. The bottom blot in (C) which was transferred from separate gels but immunoblotted and exposed together was delimited by a black line. The above experiments were performed three times with similar results.

immunity (Furniss et al., 2018). Our discovery of the DUBs UBP13, UBP24, and a UCH in the flg22-treated ubiquitylome implies that the release of Ub from targets is also a regulatory step in immune elicitation.

A common fate for ubiquitylated proteins is turnover by the 26S proteasome. This multisubunit particle consists of a 20S cylinder-shaped core protease (CP) that houses the peptidase activities, which is capped at one or both ends by the 19S regulatory particle (RP) that assist in substrate recognition, poly-Ub chain removal, unfolding, and finally translocation of the unfolded protein into to the CP for digestion (Zhou and Zeng, 2017; Marshall and Vierstra, 2018). The CP is assembled from four stacked heptameric rings of related α (PAA-PAG) and β (PBA-PBG) subunits arranged in an αββα configuration. By contrast, RP is created by a ring of six RP ATPases (RPT1-RPT6) together with a heterogeneous collection of non-ATPase subunits (RPN1-3 and RPN5-14). The RPT ring provides the unfoldase activities that prepare substrates for CP import, RPN10, RPN13, and possible RPN14/SEM1 serves as Ub receptors, and RPN11 is one of the several proteasome-bound DUBs that help release the Ub moieties prior to proteolysis. Unexpectedly, we identified PAC1 (α3), PBB1 (β2), and PBE2 (β5) within the CP, RPT3, and RPT6b within the RP ATPase ring, and RPN2b, RPN3a, RPN6, and RPN8a/b in the RP cap, as part of the flg22-induced ubiquitylome (Figure 2, B and Tables 1 and 2). Additional RPN subunits were identified (RPT1a, RPT4b, RPT5b, RPN1a, RPN7, and RPN11) in the ubiquitylome from untreated samples as well. Whereas this extensive modification of proteasomes is consistent with its ubiquitylation helping remove damaged particles via autophagy more generally (Marshall et al., 2015), and possibly as a target of during pathogen attack more specifically (Üstün et al., 2016), the preferential and rapid modification of some subunits after flg22 treatment also suggested an active host defense response. As the selective modifications of several proteasome subunits occurred within 30 min of flg22 treatment and long before any impact on 26S proteasome synthesis, we propose that they reflect early defense signaling events.

Flg22 induces UBC13 ubiquitylation and its role in plant immunity

We further connected the ubiquitylation target UBC13 (AT3G46460) to flg22 perception by studying its ubiquitylation profile and impact on pathogen defense. It should be mentioned that UBC13 is unrelated to the UBC35 and UBC36 subfamily in *Arabidopsis*, which is unfortunately also named UBC13A (AT1G78870) and UBC13B (AT1G16890), respectively (Wen et al., 2008). As shown in Figure 5, A, we confirmed that UBC13 is ubiquitylated using a UBC13-HA variant co-expressed in Arabidopsis leaf protoplasts with FLAG-Ub. Only a monoubiquitylated form was evident in the immunoprecipitates from both untreated and flg22-treated samples. Intriguingly, its abundance was slightly elevated upon flg22 exposure. Whether this addition was directed by autoubiquitylation or by a second factor (E3?) is not currently known.

To examine whether UBC13 influences immune signaling, we examined two T-DNA insertion mutants *ubc13-1* (CS389049) and *ubc13-2* (CS389056), available from the GABI-Kat collection (Kleinboelting et al., 2012). Both mutants were predicted to harbor a T-DNA sequence within the sixth exon of *UBC13*, which was confirmed by genomic PCR with gene-specific and T-DNA border primers (Supplemental Figure S1, B and C). When compared with wild-type *Arabidopsis* Col-0 leaves, homozygous *ubc13-2* leaves displayed enhanced ROS production upon flg22

Downloaded from https://academic.oup.com/plphys/article/185/4/1943/6122724 by guest on 30 April 2021

Table 2 Examples of UBQ pathway components identified from ubiquitylomes

Locus ID	Other names	Description	Category	Role in immunity	Condition	References
AT2G47110	UBQ6	Poly-UBQ gene	Ubiquitin	Not known.	flg22	
AT2G30110	UBA1	Ub-activating enzyme 1	E1	Involved in PTI and ETI.	flg22	Goritschnig et al. (2007) and Furniss et al. (2018)
AT1G78870	UBC13A, UBC35	Ub-conjugating enzyme 35/13A	E2	Regulates the immune response mediated by Fen and other R proteins through Lys-63-linked ubiquitylation	flg22	Mural et al. (2013) and Wang et al. (2019)
AT3G46460	UBC13	Ub-conjugating enzyme 13		Characterized in this study.	flg22	
AT4G02570	AXR6, CUL1	Cullin-1, a component of SCF Ub E3 ligase complexes		SKP1-CULLIN1-CPR1 (SCF), regulates protein stability of SNC1 and RPS2 and autoimmunity	flg22	Cheng et al. (2011)
AT5G46210	CUL4	CULLIN4, Ub E3 ligase		Required for *PR gene* expression and resistance to Agrobacterial infection.	flg22	Liu et al. (2012)
AT4G12570	UPL5	Ub E3 ligase UPL5	E3	Required for SA- and NPR1-mediated plant immunity	flg22	Miao and Zentgraf (2010); Zhou and Zeng (2017); and Furniss et al. (2018)
AT1G70320	UPL2	Ub E3 ligase 2		Not known	Control, flg22	
AT4G30890	UBP24	Ub-specific protease 24	UBP	Negatively regulates abscisic acid signaling; a potential MPK3 interactor.	flg22	Zhao et al. (2016) and Rayapuram et al. (2018)
AT3G11910	UBP13	Ub-specific protease 13		Negatively regulates plant resistance against *Pst* DC3000 infections	flg22	Ewan et al. (2011)
AT5G06600	UBP12	Ub-specific protease 12			Control, flg22	
AT4G24320		Ub carboxyl-terminal hydrolase family protein	UCH	Not known	flg22	
AT3G61140	CSN1, FUS6	COP9 signalosome subunit 1	COP9	Not known	flg22	
AT5G56280	CSN6A	COP9 signalosome complex subunit 6a		Not known	flg22	
AT3G22110	PAC1	26S proteasome subunit alpha type-4	Proteasome component	Both the 26S proteasome core and RPs were implicated to be involved in plant defense against pathogen infections.	flg22	Lee et al. (2006); Dielen et al. (2010); Marino et al. (2012); Yao et al. (2012); Üstün et al. (2016); and Adams and Spoel (2018)
AT3G27430	PBB1	26S proteasome subunit beta type-7A			flg22	
AT3G26340	PBE2	26S proteasome subunit beta type-5B			flg22	
AT5G58290	RPT3	26S proteasome regulatory AAA-ATPase subunit			flg22	
AT5G20000	RPT6b	26S proteasome regulatory AAA-ATPase subunit			flg22	
AT2G32730	RPN2a	26S proteasome regulatory subunit			flg22	
AT1G75990	RPN3b	26S proteasome regulatory subunit			flg22	
AT1G29150	RPN6	26S proteasome regulatory subunit			flg22	
AT3G11270	RPN8b	26S proteasome regulatory subunit			flg22	
AT1G53750	RPT1a	26S proteasome regulatory AAA-ATPase subunit			Control, flg22	

(continued)

Downloaded from https://academic.oup.com/plphys/article/185/4/1943/6122724 by guest on 30 April 2021

Table 2 Continued

Locus ID	Other names	Description	Category	Role in immunity	Condition	References
AT1G45000	RPT4b	26S proteasome regulatory AAA-ATPase subunit			Control, flg22	
AT2G20580	RPN1a	26S proteasome regulatory subunit			Control, flg22	
AT1G20200	RPN3a, EMB2719	26S proteasome regulatory subunit			Control, flg22	
AT4G24820	RPN7	26S proteasome regulatory subunit			Control, flg22	
AT5G05780	RPN8a	26S proteasome regulatory subunit			Control, flg22	
AT5G23540	RPN11	26S proteasome regulatory subunit			Control, flg22	
AT1G09100	RPT5b	26S proteasome regulatory AAA-ATPase subunit			Control	
AT1G04810	RPN2b	26S proteasome regulatory subunit			Control	
AT2G02560	CAND1, ETA2	Cullin-associated and neddylation dissociated 1	Ub component	Regulators of SCF (CPR1) complexes	flg22	Huang et al. (2016)
AT3G20620		F-box family protein-related		Not known	Control, flg22	
AT3G23633		F-box associated ubiquitylation effector family protein		Not known	Control, flg22	
AT1G77710	Ufm1, CCP2	Ub-like, Ufm1		Not known	Control	

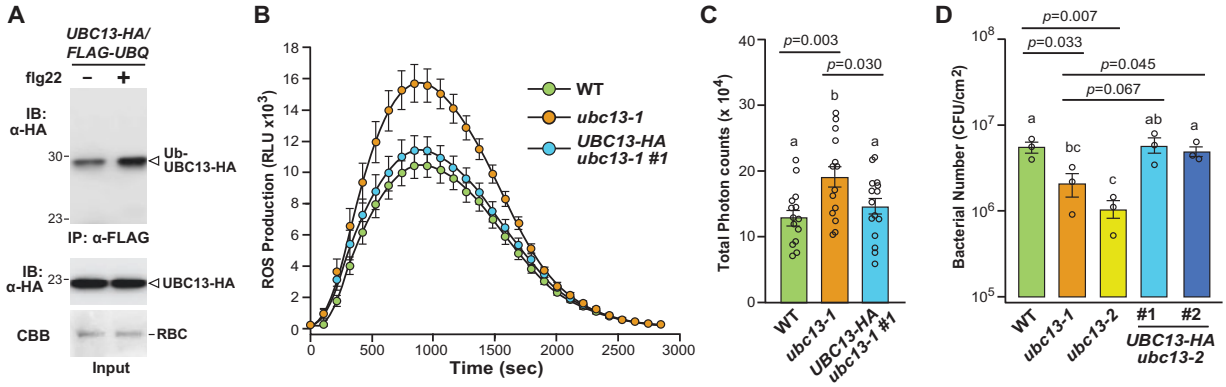

Figure 5 UBC13 is ubiquitylated and negatively regulates PTI responses. A, In vivo ubiquitylation of UBC13 upon flg22 treatment. Protoplasts were co-transfected with *FLAG-UBQ* and HA-tagged UBC13 (*UBC13-HA*) and incubated for 10 h followed by treatment with 100 nM flg22 for 30 min. Protein extracts were immunoprecipitated with anti-FLAG beads (IP: α-FLAG) and the ubiquitylated proteins were immunoblotted with anti-HA antibodies (top). The input control was shown by an anti-HA immunoblot (bottom). B and C, UBC13 negatively regulates flg22-triggered ROS production. Leaf disks of 4-week-old WT, *ubc13* (*CS389049*/*ubc13-1* and *CS389056*/*ubc13-2*), and plants harboring the *p35S:UBC13-HA* transgene in the *ubc13-2* mutant background were treated with 100 nM flg22. ROS production was monitored over time in (B). The data are shown as means ± SE overlaid on dot plot (n = 16) of RLU. The total photon count was shown in (C). Different letters above the bars indicate significant differences with $P < 0.05$. D, *ubc13* mutants have elevated resistance against *Pst* DC3000. Leaf disks of 4-week-old soil-grown WT, *ubc13-1*, *ubc13-2*, and *p35S::UBC13-HA ubc13-2* (Lines 1 and 2) plants were hand-infiltrated with *Pst* DC3000 at $OD_{600} = 5 \times 10^{-4}$ CFU/mL, and bacterial growth was counted at 3 dpi. The data are shown as means ± SE overlaid on the dot plot (n = 3). The experiments were performed three times with similar results. Different letters above the bars indicate significant differences with $P < 0.05$.

treatment, based on the chemiluminescence assay, and were significantly more resistant against *Pst* DC3000 infections (Figure 5, B–D). The involvement of UBC13 in defense responses was further confirmed in the complementation lines that harbor the *UBC13-HA* transgene. Both ROS production and disease resistance against *Pst* DC3000 infections were returned to wild-type levels in homozygous *UBC13-HA ubc13-2* plants (Figure 5, B–D). Together, our results imply

Downloaded from https://academic.oup.com/plphys/article/185/4/1943/6122724 by guest on 30 April 2021

that UBC13 negatively regulates plant immunity possibly by increasing the ubiquitylation state of UBC13.

Flg22 induces polyubiquitylation of RPN8b to potentially impact plant immunity

Our discovery that RPN8 is rapidly ubiquitylated upon treating Arabidopsis with flg22 was particularly intriguing because of its role in RP assembly where it associates with the DUB RPN11 to form an RPN11-RPN8 hetero-dimeric subcomplex (Smalle and Vierstra, 2004; Murata et al., 2009). Two paralogs of RPN8 (RPN8a and RPN8b) assemble into the 26S particle in *Arabidopsis*. Whereas the RPNA8a isoform was more highly expressed based on mRNA levels and more commonly detected within the particle by MS (Book et al., 2010), only RPN8b was identified here in flg22-treated ubiquitylome, suggesting that its modification has a selective effect on 26S proteasome structure/function. As shown in Figure 6, A, we confirmed the ubiquitylation of RPN8b by co-expressing an HA-tagged variant with FLAG-Ub in our *Arabidopsis* protoplast ubiquitylation system. Polyubiquitylated species of RPN8b-HA were evident in the immunoprecipitates from both untreated and flg22-treated samples, but their abundance was markedly enhanced upon flg22 treatment (Figure 6, A).

To test whether RPN8b contributes to immune signaling, we analyzed two T-DNA insertion mutants available from the SALK insertion collection (*rpn8b-1*, *SALK_128568* and *rpn8b-2*, *SALK_023568*). The *rpn8b-1* allele was previously shown to harbor a T-DNA sequence within the first intron (Palm et al., 2019), whereas we found that the *rpn8b-2* allele harbored a T-DNA sequence within the second intron, both of which were confirmed here by genomic PCR with gene-specific and T-DNA border primers (Supplementary Figure S1, D). When compared with wild-type *Arabidopsis* Col-0 leaves, homozygous *rpn8b-1* mutant leaves showed an increase in ROS production upon flg22 perception by the chemiluminescence assay, and enhanced disease resistance upon infiltrating leaves with *Pst* DC3000 (Figure 6, B–D). Complementation studies then connected RPN8b to the phenotypes described here; transgenic plants expressing RPN8b-HA under the control of the CaMV *35S* promoter in the *rpn8b-1* background had their levels of flg22-induced ROS production and disease resistance restored to those in wild type (Figure 6, B–D). Collectively, the data implicated RPN8b as a negative regulator of plant immunity possibly through a process that enhances its ubiquitylation state.

Mapping ubiquitylation sites on Ub conjugates

One strategy to demonstrate the impact of ubiquitylation on protein function/stability is to identify the modified lysine within the target and then block this modification through lysine to arginine substitutions. Consequently, a catalog of such sites is valuable, which can be detected by MS identification of Ub footprints, i.e. trypsin-protected lysines bearing an isopeptide linked di-glycine moiety (+114 kDa; see Figure 7, A). Directed queries of all of our MS datasets identified 64 ubiquitylation sites within 54 *Arabidopsis* proteins (Table 3), which adds to the expanding list generated by other reports (Maor et al., 2007; Saracco et al., 2009; Kim et al., 2013; Johnson and Vert, 2016; Aguilar-Hernandez et al., 2017). Interestingly, noncanonical ubiquitylation sites detected in yeast or mammals, such as those involving serine, threonine, or cysteine residues (Iwai and Tokunaga, 2009; Shimizu et al., 2010; Okumoto et al., 2011) were not identified in here. Their absence is consistent with the

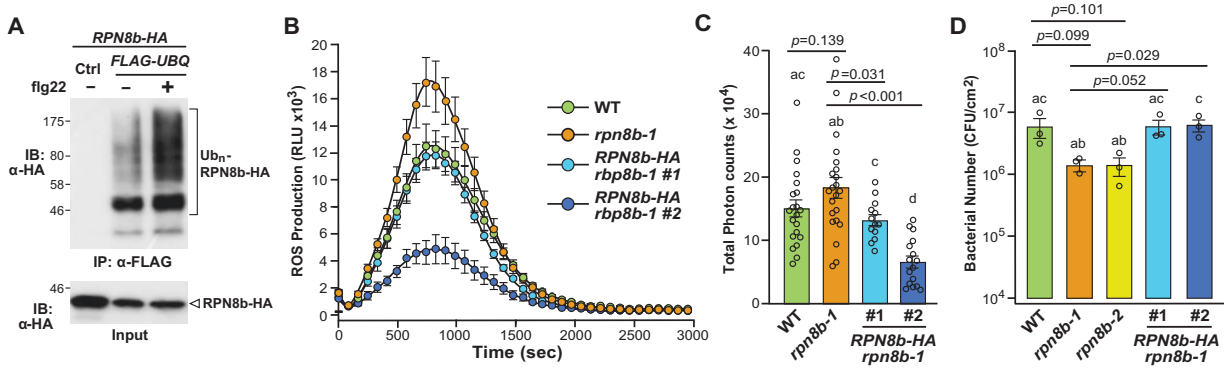

Figure 6 RPN8b is ubiquitylated and negatively regulates PTI responses. A, In vivo ubiquitylation of RPN8b upon flg22 treatment. Protoplasts were co-transfected with *FLAG-UBQ* and HA-tagged RPN8b (*RPN8b-HA*) or a control vector (Ctrl) and incubated for 10 h followed by treatment with 100 nM flg22 for 30 min. Protein extracts from protoplasts were immunoprecipitated with anti-FLAG beads (IP: α-FLAG) and the ubiquitylated proteins were immunoblotted with anti-HA antibodies (top). The input control was shown by an anti-HA immunoblot (bottom). B and C. RPN8b negatively regulates flg22-triggered ROS production. Leaf disks of 4-week-old WT, *rpn8b-1* (*SALK_128568*), *rpn8b-2* (*SALK_023568*), and *rpn8b-1* plants harboring the *p35S::RPN8b-HA* transgene were treated with 100 nM flg22 or water as a control, and ROS production was monitored over time in (B). The data are shown as means ± SE overlaid on the dot plot ($n \geq 13$) of RLU. The total photon count was shown in (C). Different letters above the bars indicate significant differences with $P < 0.05$. D, *rpn8b* mutants have elevated resistance against *Pst* DC3000. Leaf disks from 4-week-old soil-grown WT, *rpn8b-1*, *rpn8b-2*, and *35S::RPN8b rpn8b-1* plants were hand-infiltrated with *Pst* DC3000 at $OD_{600} = 5 \times 10^{-4}$ CFU/mL, and bacterial growth was counted at 3 dpi. The data are shown as means ± SE overlaid on dot plot ($n = 3$). The experiments were performed three times with similar results. Different letters above the bars indicate significant differences with $P < 0.05$.

Downloaded from https://academic.oup.com/plphys/article/185/4/1943/6122724 by guest on 30 April 2021

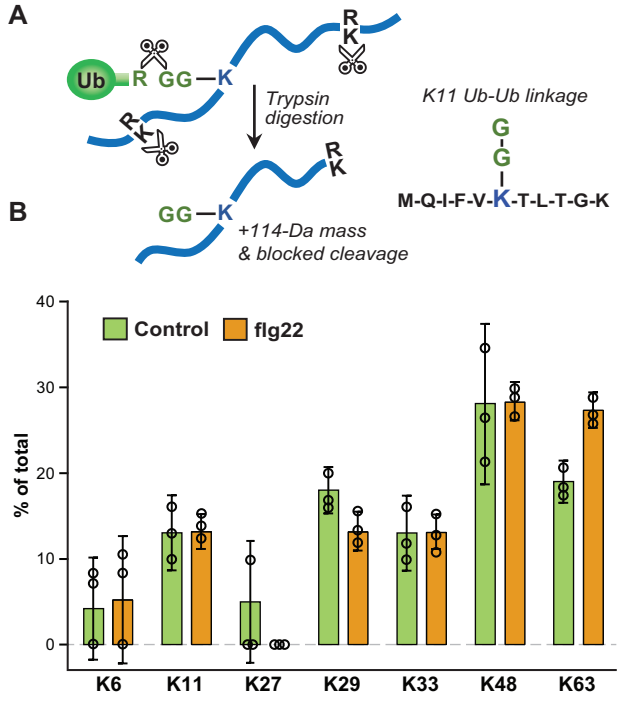

Figure 7 MS/MS mapping of Ub–Ub linkages. A, Strategy for detecting ubiquitylation sites by MS/MS. After trypsin digestion, a diglycine remnant of Ub covalently appended to a lysine residue of a conjugated protein was detected by an increased mass of 114 kDa for the lysine residue, along with protection from trypsin cleavage after that residue. Amino acids are denoted by single-letter code. B, The distribution of Ub–Ub linkages across the seven Ub lysines based on MS analysis from *Arabidopsis* transgenic plants carrying *6HIS-UBQ* seedlings treated with or without 100 nM flg22. Percentage of Ub footprints at each site was obtained from PSM counts of diagnostic footprint peptides.

previous ubiquitylome studies (Kim et al., 2013) and implies that these linkages are rarely, if at all, used by plants.

Analysis of poly-Ub linkages

Owing to the widespread observations that poly-Ub chains of various linkages confer unique functions to Ub (Vierstra, 2009; Komander and Rape, 2012), we examined how flg22 treatment might affect the abundances of these polymers, using the diagnostic Ub footprint peptides for quantification based on peptide spectral matches (Peng et al., 2003). Whereas footprints on each of the seven internal lysines (K6, K11, K27, K29, K33, K48, and K63) were identified (Figure 7, B), none were seen using the N-terminal methionine, which would have signified linear Ub concatemers (Iwai and Tokunaga, 2009). K48-linked Ub–Ub connections were the most abundant and comprised ~30% of the total detected linkages in both control and flg22-treated samples (Figure 7, C). The second most abundant linkage involved K63 and was followed in abundance by those involving K29, K11, K33, K6, and K27 (Figure 7, B). Interestingly, flg22 exposure altered the relative abundance of poly-Ub linkages; the percentages of K63 linkages increased, whereas the percentages of K27 and K29 linkages decreased (Figure 7, B). The biological relevance of such changes awaits further study, but it is interesting to note connections between K63 Ub chains and endosomal sorting (Johnson and Vert, 2016), and the important roles of protein trafficking to pathogen defense (Zhou and Zeng, 2017).

Discussion

Protein ubiquitylation is involved in nearly all aspects of eukaryotic biology, leading to a multitude of distinct signals within a variety of cellular and physiological contexts. In line with prior studies with yeast and mammals (Bennett et al., 2007; Ordureau et al., 2020), we show here and elsewhere (Aguilar-Hernandez et al., 2017) that dynamic and multifaceted changes in the plant ubiquitylome also occur. By employing a genetically encoded *hexa-6HIS-UBQ* variant coupled with an improved two-step enrichment protocol for ubiquitylated proteins, followed by deep LC–MS/MS analysis, we found profound and complex protein ubiquitylation patterns upon immune elicitation in Arabidopsis.

We propose that the use of two affinity-purification steps, with the second under strongly denaturing conditions, are essential to generate reliable catalogs, which resulted here in the detection of 690 possible substrates along with 64 ubiquitylation sites mapped onto 54 individual proteins. Among the 10 candidate proteins that we subsequently tested by in vivo conjugation assays, all were confirmed as ubiquitylated targets in planta. Whereas it is possible that the ubiquitylated species seen in protoplasts were artifacts derived from ectopic expression, the fact that different types of linkages were seen (mono- versus polyubiquitylation) and that both increased and decreased responses were seen soon after flg22 elicitation argue otherwise.

We also identified Ub–Ub linkages involving all seven lysine residues based on the discovery of diagnostic footprint peptides, with those involving K48 and K63 being the most abundant. Whereas K48 polyubiquitylation has been linked to 26S proteasome-mediated turnover, and K63 ubiquitylation has been connected to the endocytic internalization of plasma membrane proteins (Romero-Barrios and Vert, 2018), the functions of the other poly-Ub linkages remain largely unknown in *Arabidopsis*, even though the total abundance of those linkages exceeds 40% of the total. In addition, we saw an increased number of ubiquitylated proteins (391 of control versus 570 of flg22-treated) upon immune elicitation. Although the datasets were not derived from quantitative proteomic approaches, a nearly 50% increase in the number of ubiquitylated proteins seen soon after immune elicitation suggests a strong activation of the machinery that supports Ub transfer.

Notably, our flg22-induced datasets were obtained using seedlings treated for only 30 min, thus implicating ubiquitylation as an early step in immune signaling. Surprisingly, several resistance proteins known to be ubiquitylation such as FLS2, BRI1, and BIK1 were not identified here (Lu et al., 2011; Zhou et al., 2018; Ma et al., 2020), which might be explained by the nature of the tissues examined or the

Downloaded from https://academic.oup.com/plphys/article/185/4/1943/6122724 by guest on 30 April 2021

Table 3 Examples of candidates with Ub-footprints identified from ubiquitylomes

Locus ID	Other names	Description	Ub-footprint peptide	Ub-attachment sites	Condition
At1g02305	CATHB2	Cathepsin B-like protease 2	[R].GTNECGIEHGVVAGLPSDRNVVkGITTSDDLLVSSF	Lys349 of 362	Control
At1g12150	DUF827	Weak chloroplast movement under blue light protein	[K].AIEEMKQATELAQkSAESAEAAk.[R]	Lys520 of 548/Lys559 of 548	flg22
At1g26120	ICMEL1	Isoprenylcysteine methylesterase-like protein 1	[R].LPPFILFHGTDDYSIPSDASkSFAETLQR.[L]	Lys397 of 476	Control
At1g51000	At1g51000	Uncharacterized protein	[K].kITGMTTkLDELLEMMK.[E]	Lys45 of 72/Lys52 of 72	flg22
At1g55860	UPL1	Ubiquitin-protein ligase 1	[R].NIWSHSkWLVDTLQNYCR.[A]	Lys1150 of 3681	Control
At1g66760	At1g66760	MATE efflux family protein	[K].KSIETPLLLNTkQSQDEDK.[E]	Lys14 of 482	Control
At1g67980	CCOAMT	Caffeoyl-CoA 3-*O*-methyltransferase	[K].kAGVDHkINFIHSDGLK.[A]	Lys47 of 164/Lys53 of 164	flg22
At1g70320	UPL2	Ubiquitin-protein ligase 2	[R].NLWSHSkWLVDTLQNYCR.[A]	Lys1152 of 3658	Control
At1g78820	At1g78820	D-mannose binding lectin protein with Apple-like carbohydrate-binding domain-containing protein	[K].LVSRTSDMNGSDGPYSMVLDNkGLTMYVNK.[T]	Lys204 of 455	Control
At2g03810	At2g03810	18S pre-ribosomal assembly protein gar2-like protein	[K].TEEPkQGEEKLSSVSTTTSQEPNK.[T]	Lys305 of 439	Control
At2g04540	mtKAS	Beta-ketoacyl-ACP synthase, mitochondrial	[R].TGVSIGGGIGSICDIVEAAQLICEkRLR.[R]	Lys170 of 461	flg22
At2g17150	NLP1	NIN-like protein 1	[R].VDIGPSTESASTGGGNMLSSRRPGEk.[K]	Lys600 of 909	flg22
At2g18760	CHR8	Chromatin remodeling 8	[K].NGISAGLSSGkAPSSAELLNR.[I]	Lys1135 of 1246	flg22
At2g22270	At2g22270	Hematological/neurological-like protein	[K].kPTTLNEAAKQK.[E]	Lys52 of 328	flg22
At2g24030	At2g24030	Zinc ion binding/nucleic acid binding protein	[R].SLNADPGQkESVSLAMDDTQGK.[V]	Lys435 of 455	flg22
At2g25520	At2g25520	Drug/metabolite transporter superfamily protein	[K].ALMPVAVYSIGVLLk.[K]	Lys134 of 347	flg22
At2g41290	SSL2	Strictosidine synthase-like 2	[K].WISISEVEEkDGTLWVGSVNTPFAGMYKI.	Lys357 of 376	Control
At2g46535	At2g46535	Uncharacterized protein At2g46535	[R].AGDNINENNMkIMK.[F]	Lys130 of 175	flg22
At3g01460	MBD9	Methyl-CpG-binding domain-containing protein 9	[K].DYRKLECLSAEMk.[K]	Lys1267 of 2176	Control
At3g03330	At3g03330	NAD(P)-binding Rossmann-fold superfamily protein	[K].VTVVCPGPIETWNGTGTSTSEDSkSPEK.[R]	Lys246 of 328	flg22
At5g17920	MS1	Cobalamin-independent methionine synthase 1	[R].kYTEVKPALK.[N]	Lys739 of 765	flg22
At3g03780	MS2	Cobalamin-independent methionine synthase 2	[R].KYTEVkPALK[A].	Lys744 of 765	flg22
At3g13990	At3g13990	Dentin sialophosphoprotein, putative	[K].kEDTVFVEPANIkkPLENVTSEVK.[V]	Lys73 of 848/Lys85 of 848/Lys86 of 848	flg22
At3g17710	At3g17710	F-box protein	[R].LSDSLQEGYYQAAIYECASQAFkFIDTPNPFNLWPNK.[D]	Lys181 of 368	flg22
At3g17930	DAC	Defective accumulation of cytochrome B/F complex	[R].LESLSEAELEALMAQVDEEkTK.[V]	Lys186 of 190	flg22; Control
At3g25500	AFH1	Formin-like protein 1	[R].VCkEVGMINERTMVSSAHK.[F]	Lys989 of 1051	flg22
At3g46790	CRR2	Chlororespiratory reduction 2	[K].GVLYELETEEkER.[I]	Lys582 of 657	flg22; Control
At3g48100	ARR5	Two-component response regulator ARR5	[R].ELEANDIYSQLkRAK.[I]	Lys180 of 184	flg22; Control
At3g57180	BPG2	Brassinazole insensitive pale green 2	[R].ASELGTWEEkEIQVSGNSWDVK.[S]	Lys559 of 660	Control
At3g59730	LECRK-V.6	L-type lectin-domain containing receptor kinase V.6	[K].LMRLSIVYSHPDTkLDVTLCPAEFLVPPR.[K]	Lys192 of 523	flg22
At4g01550	NAC069	NAC domain-containing protein 69	[R].ATSPTALEFEkPGQENFFGMSVDDLGTPK.[N]	Lys192 of 457	Control
At4g15830	At4g15830	ARM repeat superfamily protein	[K].LSKQPEIGLNDENNPVAVAESTVEYVASENLkPFSDPESSVQR.[L]	Lys54 of 296	flg22
At4g16450	At4g16450	NADH-ubiquinone oxidoreductase	[K].GPSMVTGGLIGLMGGFMYAYQNSAGRLMGFFPNDGEVASYQk.[R]	Lys100 of 106	flg22
At4g18020	APRR2	Pseudo-response regulator 2	[K].EDETKPINkSSGIK.[N]	Lys282 of 535	flg22
At4g27595	At4g27595	Encodes a microtubule-associated protein	[K].QLEENNHALHEAELGNATLkEK.[V]	Lys349 of 1199	flg22
At4g30020	At4g30020	PA-domain containing subtilase family protein	[K].MVSANDVLLGSSGMkYNPSDCQKPEVLNk.[K]	Lys413 of 816/Lys427 of 816	flg22
At4g32390	At4g32390	Nucleotide-sugar transporter family protein	[K].ALMPVAVYSIGVLLk.[K]	Lys134 of 350	flg22
At4g33280	ARF36	Auxin response factor 36	[R].RELSNDNLDQkADVEMISAGSNk.[K]	Lys269 of 398/Lys257 of 398	flg22; Control
At4g35685	At4g35685	DNA-directed RNA polymerase III subunit	[K].LDVFEkLESK.[F]	Lys118 of 178	flg22
At4g38270	GAUT3	Galacturonosyltransferase 3	[K].ANHPSSISAGADNLkYRNPK.[Y]	Lys470 of 676	flg22; Control
At5g03610	At5g03610	GDSL esterase/lipase	[K].NkGSNPGSTRFESPLKPCCVGVSR.[E]	Lys282 of 359	flg22
At5g04550	DUF668	Type-1 restriction enzyme mjaxp r protein	[K].FYSGQLGkITSKSGPLIGMGK.[N]	Lys329 of 599	flg22; Control
At5g05560	APC1	Pollen calcium-binding protein 1	[K].kVGACSYVDDPVGCQSLLSRAMHK.[V]	Lys1542 of 1807	flg22
At5g09900	RPN5A	26S proteasome regulatory subunit, putative	[K].QVVTMEVIQWTSLWNkYkDEFEK.[E]	Lys313 of 462/Lys315 of 462	flg22

(continued)

Downloaded from https://academic.oup.com/plphys/article/185/4/1943/6122724 by guest on 30 April 2021

Table 3 Continued

Locus ID	Other names	Description	Ub-footprint peptide	Ub-attachment sites	Condition
At5g12420	WSD7	Diacylglycerol *O*-acyltransferase	[R].VFQSPGIDLCAVTIMGFkTK.[I]	Lys32 of 480	flg22
At5g19210	At5g19210	P-loop containing nucleoside triphosphate hydrolases superfamily protein	[R].DVVHVHVSAIMPMPLCLLHRFVMCEkTNK.[H]	Lys312 of 472	flg22; Control
At5g36150	PEN3	Pentacyclic triterpene synthase 3	[K].NYIPLEGNkTDVVNTGQALMVLIMGGQMDRDPLPVHR.[A]	Lys677 of 760	flg22
At5g40000	At5g40000	P-loop containing nucleoside triphosphate hydrolases superfamily protein	[R].SIEFEHPASFQTLAmDPkk.[k]	Lys214 of 470/Lys215 of 470	flg22
At5g43390	At5g43390	Uncharacterized protein	[K].kSTISGDMEDRILETAEETGGPVGK.[V]	Lys178 of 643	Control
At5g43840	HSFA6A	Heat stress transcription factor A6A	[K].VTEVkQEMMMNFLLk.[K]	Lys165 of 282/Lys175 of 282	Control
At5g52840	At5g52840	NADH-ubiquinone oxidoreductase-like protein	[K].TLEGLIAESKTEIPAATPSDPQLkE.	Lys168 of 169	flg22; Control
At5g53460	GLT1	NADH-dependent glutamate synthase 1	[K].DAFAELKNMAAASSkEEMSGNGVAAEARPSK.[V]	Lys1679 of 2208	Control
At5g55660	At5g55660	DEK domain-containing chromatin associated protein	[K].ADDGVSGVATEEDAVMKESVESADNkDAENPEGEQEK.[E]	Lys133 of 778	flg22
At5g62970	At5g62970	Protein with RNI-like/FBD-like domain	[K].IATISIGYGLDPQQKLkMEMDVK.[F]	Lys429 of 449	flg22

extraction method used, which possibly preferred cytoplasmic versus plasma membrane/organelle-associated proteins. Furthermore, we should also emphasize that the TUBE affinity approach likely binds polyubiquitylated proteins better than monoubiquitylated proteins and thus reduced the latter in our catalogs. One strategy to avoid this complication is to enrich for Ub footprints directly from trypsin-digested cell lysates using an anti-K-ε-GG antibodies specific for the GG-remnant on ubiquitylated lysines (Udeshi et al., 2013). In fact, recent studies with such antibodies in rice (*Oryza sativa*) discovered 1,376 possible ubiquitylated proteins and revealed strong changes in ubiquitylation after a 3-h exposure to flg22 or fungal chitin (Chen et al., 2018). The only complications were that designation of a protein as a Ub target was often based on a single Ub footprint peptide and the reliability of the anti-K-ε-GG antibodies. Clearly, further advancements in enrichment strategies and MS instrumentation should further expand the specificity, stringency, and depth of the ubiquitylome during diverse physiological conditions.

Within the flg22-induced ubiquitylomes identified here, we confirmed several Ub targets by in vivo ubiquitylation assays in protoplasts. Surprisingly, we found distinct ubiquitylation patterns and dynamic temporal responses to flg22 treatment. For example, MKK5 and MPK3 were strongly monoubiquitylated whereas SOBIR1 and EDS1 were mainly polyubiquitylated. Ubiquitylation of RPN8b and MPK3 was increased by flg22, with MPK3 modification showing a transient effect. By contrast, ubiquitylation of EDS1 in the protoplasts was reduced in response to flg22 treatment. In addition, receptor protein kinase RKL1 was polyubiquitylated. Although it remains unknown whether RKL1 participates in plant immunity, its close homolog RLK902 was previously shown to positively regulate plant disease resistance (Zhao et al., 2019).

Ubiquitylation often intertwines with phosphorylation in regulating protein function (Reyes et al., 2011; Hu and Sun, 2016; Skubacz et al., 2016). A well-known example in plant disease resistance is BIK1, which is phosphorylated and subsequently monoubiquitylated upon flg22 perception (Ma et al., 2020). Here, we found that the phosphorylation (Asai et al., 2002) target MPK3 is also ubiquitylated dynamically, and like phosphorylation, this modification was enhanced ~10 min after flg22 treatment, and then was reduced to basal levels after 30 min. The cognate E3 ligase for MPK3 is currently unknown; given that MPK3 phosphorylates the E3 ligase PUB22 and regulates its turnover (Furlan et al., 2017), it is possible that PUB22 directs MPK3 ubiquitylation thus creating an internal regulatory loop. As MPK3 remained unchanged despite the dynamics of its ubiquitylation after flg22 treatment, its ubiquitylation might not commit MPK3 to turnover but confer a reversible, non-proteolytic function. In line with some ubiquitylation events being reversible,

Downloaded from https://academic.oup.com/plphys/article/185/4/1943/6122724 by guest on 30 April 2021

we note the detection of several DUBs in our flg22-treated ubiquitylome datasets.

Pathway analysis of our ubiquitylome datasets upon MAMP perception revealed robust changes in the ubiquitylation status for numerous components involved in the UPS, including E1, E2, E3, and DUB family members. The in vivo ubiquitylation assays further confirmed that the E2 UBC13 in monoubiquitylated in vivo with the abundance of this modification increased modestly upon flg22 treatment. Whereas *ubc13* mutants morphologically resembled WT plants, they displayed an enhanced flg22-induced ROS burst and increased resistance against bacterial infection. Several E3s have also been implicated in immunity, including CPR1 (Gou et al., 2009, 2012; Cheng et al., 2011), PUB12/13 (Lu et al., 2011; Liao et al., 2017), PUB25/26 (Wang et al., 2018), PUB22/23/24 (Stegmann et al., 2012), and RHA3A/B (Ma et al., 2020). While it is generally accepted that E3s rather than E2s are the key determinants in substrate selection, it is possible that UBC13 preferentially works with those E3s involved in immunity.

Proteasome components, including both the core and RPs, were enriched in our ubiquitylome analysis, which is consistent with the observation in yeast (Peng et al., 2003), and the known role of ubiquitylation in directing proteasome turnover through autophagy (Marshall et al., 2015). Strikingly, several of the ubiquitylated subunits were only found in the flg22-treated ubiquitylome, implying an active regulation of the proteasome machinery upon MAMP perception. Previous studies showed that several RP subunits, such as RPN1a, RPN8a, and RPT2a, but not others, play a positive role in immunity (Yao et al., 2012). Unexpectedly, we found RPN8b negatively regulates the flg22-induced ROS burst and disease resistance against *Pst* DC3000 infection. As Arabidopsis also encodes a second isoform of RPN8 (RPN8a) that appears more dominant in providing this subunit (Book et al., 2010), one intriguing possibility is that the RPN8b isoform associates with a unique subset of proteasomes with functions more directed toward immune perception. The immunoproteasome assembled with unique isoforms of the CP subunits β1, β2, and β5 could serve as an example of such non-redundancy (Finley, 2009). Clearly, further comparisons of mutants impacting both RPN8a and RPN8b with respect to pathogen resistance, along with assays testing the ubiquitylation status of each, are now necessary to explore this notion.

Materials and methods

Plant materials and growth conditions

Arabidopsis thaliana 6HIS-UBQ transgenic plants in the Col-0 background were described previously (Saracco et al., 2009). The *ubc13-1* (*CS389049*), *ubc13-2* (*CS389056*), *rpn8b-1* (*SALK_128568*), and *rpn8b-2* (*SALK_023568*) T-DNA insertion lines were obtained from ABRC. *p35S::UBC13-HA* transgenic plants in the *ubc13-2* background and *p35S::RPB8b-HA* transgenic plants in the *rpn8b-1* background were generated in this study (see below for details). All *Arabidopsis* plants were grown in soil (Metro Mix 366, Sunshine LP5, or Sunshine LC1) in a growth chamber at 20°C–23°C, 50% relative humidity, and 75 μE m^{-2} s^{-1} light with a 12-h light/12-h dark photoperiod for 4 weeks before pathogen infection assay, protoplast isolation, and ROS assays.

Plasmid construction and generation of transgenic plants

MPK3-HA, *MKK5-MYC*, and *FLAG-UBQ* in the plant gene expression vector *pHBT* used for protoplast assays were described previously (Asai et al., 2002; Lu et al., 2011). SOBIR1, RKL1, UBC13, RPN8b, and EDS1 tagged with HA in the *pHBT* vector were generated as following: the gene was PCR amplified from total Col-0 cDNA with primers containing *Bam*HI (for *SOBIR1*, *RKL1*, *UBC13*, and *RPN8b*) or *Nco*I (for *EDS1*) at the 5′-end and *Stu*I at the 3′-end, followed by *Bam*HI/*Nco*I and *Stu*I digestion and ligation into the *pHBT* vector with a sequence encoding a HA tag at the 3′-end. DNA fragments cloned into the *pHBT* vectors were confirmed as correct by Sanger sequencing. The *UBC13-HA* and *RPN8b-HA* transgenes were further shuttled into a *pCB302* vector by insertion into *Bam*HI and *Stu*I digestion sites. The *A. tumefaciens*-mediated floral dip was used to transform the above binary vectors into *ubc13-2* or *rpn8b-1* plants. Transgenic plants were selected by glufosinate-ammonium (Basta, 50 μg/mL) resistance. Multiple transgenic lines were analyzed by immunoblotting for protein expression. Two lines with a 3:1 segregation ratio for Basta resistance in the T3 generation were selected to obtain homozygous seeds for further studies.

Affinity purification of ubiquitylated proteins

Affinity purification of ubiquitylated proteins was described (Kim et al., 2013) with modifications. Seeds of *Arabidopsis* Col-0 and *6HIS-UBQ* transgenic plants were vernalized at 4°C for 3 d and surface sterilized with 75% (v/v) ethanol for 10 min and 5% (v/v) bleach for 10 min, and plated in 0.5-strength Murashige and Skoop (MS) medium containing 1% (w/v) sucrose and 0.5% (w/v) agar (100 seedlings per plate) were grown at 23°C under 75 μE m^{-2} s^{-1} light with a 12-h light/12-h dark photoperiod for 14 d. Approximately 5,000 seedlings (50 plates) were used for each biological replicate which generated ∼16–21 g fresh weight of tissue. Seedlings were gently transferred into a Petri dish plate and incubated overnight in water. After removing the water by vacuum, seedlings were treated for 30 min with 100 nM flg22 or water as a control.

Seedlings were gently blot-dried on Kimwipes, frozen to liquid nitrogen temperatures, and homogenized in 0.5 g/mL of extraction buffer (EB; 50 mM Tris–HCl, pH 7.2, and 200 mM NaCl), containing 0.25% (v/v) Triton X-100, 1× protease inhibitor cocktail (Roche, 1 tablet per 10 mL of EB), 2 mM phenylmethanesulfonyl fluoride, 10 mM 2-chloroacetamide, 10 mM sodium metasulfite, and 1 mM *N*-ethylmaleimide (freshly added). The homogenate was filtered through two layers of Miracloth and the supernatant was mixed with TUBEs beads as the ratio of 40 g of tissue to 1 mL of

Downloaded from https://academic.oup.com/plphys/article/185/4/1943/6122724 by guest on 30 April 2021

beads. After incubation for 6 h at 4°C, the beads were collected in a 2 × 1-cm chromatography column and washed three times with EB and three times with EB plus 2 M NaCl, and eluted in 10 mL of 7 M guanidine-HCl, 100 mM NaH_2PO_4, and 10 mM Tris–HCl (pH 8.0, 24°C). The eluted conjugates were incubated with 500 µL of Ni-NTA beads for 12 h at 4°C in the same buffer with the addition of 20 mM imidazole and 10 mM 2-chloroacetamide. The beads were collected and washed once in 6 M guanidine-HCl, 0.1% (w/v) SDS, 100 mM NaH_2PO_4, and 10 mM Tris–HCl (pH 8.0), and once in urea buffer (UB; 8 M urea, 100 mM NaH_2PO_4, and 10 mM Tris–HCl [pH 8.0]) also containing 0.1% (v/v) Triton X-100, twice in UB plus 20 mM imidazole, and three times in UB alone, and eluted by 1 mL of UB supplemented with 400 mM imidazole. The two-step purified conjugates were filtered by the Ultracel-10K filter (Millipore) and separated by SDS–PAGE followed by staining for protein with silver, or immunoblotting with anti-Ub (Sigma–Aldrich) or anti-His (Novagen) antibodies to detect Ub conjugates.

Mass spectrometry

Purified proteins (100 µL) or control samples were reduced with 10 mM DTT at room temperature for 1 h, and alkylated in the dark in the presence of 30 mM 2-chloroacetamide at room temperature for a further 1 h. Excess alkylating agent was quenched with 20 µL of 200 mM DTT for 10 min. Samples, 10-fold diluted with 25 mM ammonium bicarbonate, were digested for 12 h at 37°C with 2 mg of sequencing-grade trypsin (Promega), followed by a second incubation for 6 h with an additional 2 mg of trypsin. Digestion products were desalted using a C18 solid-phase extraction pipette tip (SPEC PT C18, Varian), vacuum dried, and reconstituted in 10 µL of 0.1% (v/v) formic acid and 5% (v/v) acetonitrile in water for MS analysis.

Samples were analyzed by a nanoflow LC system (nanoAcquity; Waters) combined with an electrospray ionization FT/ion-trap mass spectrophotometer (LTQ Orbitrap Velos; Thermo Fisher Scientific). The LC system employed a 100 × 365-µm fused silica microcapillary column packed with 15 cm of 3 µm diameter, 100 Å pore size, C18 beads (Magic C18; Bruker), with the emitter tip pulled to 2 mm using a laser puller (Sutter Instruments). Peptides were loaded onto the column for 30 min at a flow rate of 500 nL/min and eluted over 120 min at a 200-nL/min flow rate with a gradient of 2%–30% (v/v) acetonitrile in 0.1% (v/v) formic acid. MS spectra were acquired in the FT orbitrap between 300 and 1,500 mass-to-charge ratios (m/z) at a resolution of 60,000, followed by 10 MS/MS HCD scans of the 10 highest intensity parent ions at 42% relative collision energy and 7,500 resolution, with a mass range starting at 100 mass-to-charge ratios. Dynamic exclusion was enabled with a repeat value of 2 for 30 s and an exclusion window for 120 s.

MS data analysis

The MS/MS data were searched using SEQUEST version 1.2 (ThermoFisher Scientific) against the *A. thaliana* ecotype Col-0 protein database (IPI database, version 3.85, containing 39,677 entries available within the *Arabidopsis* Information Resource [TAIR], http://www.arabidopsis.org) database. Masses for both precursor and fragment ions were treated as monoisotopic. Met oxidation (+15.994915 Da), Cys carbamidomethylation (+57.021464 Da), the di-Gly Ub footprint indicating Ub addition to a lysine residue (+114.043 Da) were set as variable modifications. The database search allowed for up to two missed trypsin cleavages, and the ion mass tolerances were set to 10 ppm for precursor and 0.1 Da for HCD fragments. The data were filtered using a 1% FDR and a minimum of two peptide matches was required or at least one peptide if it included a diGly Ub footprint.

For a focused search for Ub attachment sites and other PTMs, the MS/MS data were searched using Proteome Discoverer (version 2.0.0.802; Thermo Fisher Scientific) with peptide assignment completed by SEQUEST HT (Eng et al., 1994) against the *Arabidopsis* ecotype Col-0 protein database (Araport11 containing 40,782 entries available within the *Arabidopsis* Information Resource [TAIR] database). Trypsinized peptides with a predicted ubiquitylated lysine at the C-terminal end were considered erroneous based on the assumption that a Ub addition precludes digestion after that residue. Only "Master Proteins" were included in the final dataset.

GO analysis was evaluated by DAVID Functional Annotation Tool (Huang da et al., 2009) using GO annotations in the TAIR GO database (http://www.arabidopsis.org/). Fold enrichments were calculated based on the frequency of proteins annotated to the term compared with their frequency in the proteome. The *P*-value combined with the FDR correction was used as criteria of significant enrichment for GO catalogs, whereas a *P*-value < 0.05 was considered to be enriched for GO terms. The GO annotation was classified based on the "biological processes," "molecular functions," and "cellular components" categories and visualized as a bubble plot by R Project 4.0.0 (https://www.r-project.org/; Bonnot et al., 2019). Protein interaction networks were created by the STRING database version 11.0 (Szklarczyk et al., 2015), and visualized by Cytoscape version 3.8.0 (Shannon et al., 2003).

Detection of ROS production

Leaves from 4- to 5-week-old, soil-grown *Arabidopsis* plants were punched into 5-mm diameter discs. The discs were incubated in 100 µL of water with gentle shaking overnight, which was then replaced with 100 µL of reaction solution containing 50 µM luminol and 10 µg/mL horseradish peroxidase (Sigma–Aldrich) supplemented with or without 100 nM flg22. Luminescence was measured with a luminometer (GloMax-Multi Detection System, Promega) with a setting of 1 min as the interval for 40 min. Detected values for ROS production were indicated as means of relative light units (RLUs).

Downloaded from https://academic.oup.com/plphys/article/185/4/1943/6122724 by guest on 30 April 2021

Pathogen infection assays

Pseudomonas syringae pv. *tomato* (*Pst*) DC3000 was cultured for overnight at 28°C in King's B medium supplemented with rifamycin (50 μg/mL). Cells were collected by centrifugation at 903 × *g*, washed, and re-suspended to the density of 5 × 10^5 cfu/mL in 10 mM $MgCl_2$. Leaves from 4-week-old *Arabidopsis* plants were hand-inoculated with bacterial suspension using a needleless syringe. To measure in planta bacterial growth, three to four samples, each containing two 6-mm diameter leaf discs, were homogenized in 100 μL of water, and plated in serial dilutions on medium containing 1% (w/v) tryptone, 1% (w/v) sucrose, 0.1% (w/v) glutamic acid, 1.8% (w/v) agar, and 25 μg/mL rifamycin. Plates were incubated at 28°C and bacterial colony forming units (cfu) were counted after 2 d.

In vivo ubiquitylation assays

Protoplast isolation and transient expression assay were as described previously (ZHou et al., 2014). Protoplasts were freshly isolated from leaves of 4-week-old Col-0 plants and transfected at 2 × 10^5 cell/mL (500 μL) with various combinations of plasmids harboring genes encoding FLAG-UBQ (25 μL at 2 μg DNA/μL), and the HA- or Myc-tagged proteins of interested (25 μL at 2 μg DNA/μL). The protoplasts were incubated for overnight at room temperature followed by a 2-h treatment with DMSO alone or 2 μM MG132 dissolved in DMSO, and then a 2-h exposure to 100 nM flg22. After homogenization in 300 μL of IP buffer (150 mM NaCl, 50 mM Tris–HCl [pH 7.5], 5 mM Na_2EDTA, 1% (v/v) Triton X-100, 2 mM Na_3VO_4, 2 mM NaF, 1 mM DTT, and 1:100 diluted protease inhibitor cocktail (Sigma–Aldrich)], the FLAG-tagged proteins were immunoprecipitated by incubation of the extracts with 5 μL of anti-FLAG antibody agarose beads (Sigma–Aldrich) for 1 h at 4°C with gentle shaking. The anti-FLAG antibody beads were collected and washed three times with IP buffer (without cocktail) and once with 50 mM Tris–HCl (pH 7.5), and then incubated in 30 μL of hot SDS-PAGE sample buffer for 5 min. Twenty microliters of the sample before adding the beads was used as the input control. The samples were separated by SDS–PAGE followed by electrophoretic transfer onto polyvinylidene difluoride (PVDF) membranes (Bio-Rad), and immunoblotting with appropriate antibodies. Antibodies against plant Ub (van Nocker et al., 1996) and 6His (Kim et al., 2013) were as described. Anti-FLAG, anti-HA, and anti-Myc antibodies were purchased from Sigma–Aldrich (A8592), Roche (12013819001), and Santa Cruz (sc-40), respectively.

Statistical analyses

Data for quantification analyses are presented as means ± standard error of the mean (SE). The statistical analyses were performed by Student's *t* test or one-way analysis of variance (ANOVA) test (*P value < 0.05, **P value < 0.01, ***P value < 0.001). The number of replicates is shown in the figure legends.

Accession numbers

Sequence data from this article can be found in the GenBank/EMBL data libraries under the accession numbers listed in Tables 1, 2, or Supplemental Table S1.

Supplemental data

The following supplemental materials are available.

Supplemental Figure S1. Mutants genotyping PCR.

Supplemental Table S1. Full list of proteins identified in the ubiquitylome analysis.

Acknowledgments

The authors thank the *Arabidopsis* Biological Resource Center (ABRC) for T-DNA insertion mutant seeds, and members of the laboratories of L.S., P.H., and R.D.V. for discussions and comments of the experiments.

Funding

This work was supported by grants from the National Institutes of Health (NIH; R01-GM092893) and National Science Foundation (NSF; MCB-1906060) to P.H., NIH (R01-GM097247) and the Robert A. Welch Foundation (A-1795) grant to L.S., and a grant from the NIH (R01-GM124452) to R.D.V. C. Z. and Y.H. were partially supported by the China Scholarship Council (CSC).

Conflict of interest statement. The authors declare no conflict of interests.

References

Adams EHG, Spoel SH (2018) The ubiquitin–proteasome system as a transcriptional regulator of plant immunity. J Exp Bot **69**: 4529–4537

Aguilar-Hernandez V, Kim DY, Stankey RJ, Scalf M, Smith LM, Vierstra RD (2017) Mass spectrometric analyses reveal a central role for ubiquitylation in remodeling the Arabidopsis proteome during photomorphogenesis. Mol Plant **10**: 846–865

Albert I, Böhm H, Albert M, Feiler CE, Imkampe J, Wallmeroth N, Brancato C, Raaymakers TM, Oome S, Zhang H (2015) An RLP23–SOBIR1–BAK1 complex mediates NLP-triggered immunity. Nature Plants **1**: 1–9

Asai T, Tena G, Plotnikova J, Willmann MR, Chiu WL, Gomez-Gomez L, Boller T, Ausubel FM, Sheen J (2002) MAP kinase signalling cascade in Arabidopsis innate immunity. Nature **415**: 977–983

Bakker EG, Toomajian C, Kreitman M, Bergelson J (2006) A genome-wide survey of R gene polymorphisms in Arabidopsis. Plant Cell **18**: 1803–1818

Bellati J, Champeyroux C, Hem S, Rofidal V, Krouk G, Maurel C, Santoni V (2016) Novel aquaporin regulatory mechanisms revealed by interactomics. Mol Cell Proteomics **15**: 3473–3487

Bennett EJ, Shaler TA, Woodman B, Ryu KY, Zaitseva TS, Becker CH, Bates GP, Schulman H, Kopito RR (2007) Global changes to the ubiquitin system in Huntington's disease. Nature **448**: 704–708

Bethke G, Pecher P, Eschen-Lippold L, Tsuda K, Katagiri F, Glazebrook J, Scheel D, Lee J (2012) Activation of the *Arabidopsis thaliana* mitogen-activated protein kinase MPK11 by the flagellin-derived elicitor peptide, flg22. Mol Plant Microb Interact **25**: 471–480

Downloaded from https://academic.oup.com/plphys/article/185/4/1943/6122724 by guest on 30 April 2021

Böhm H, Albert I, Fan L, Reinhard A, Nürnberger T (2014) Immune receptor complexes at the plant cell surface. Curr Opin Plant Biol **20**: 47–54

Bonnot T, Gillard M, Nagel D (2019) A simple protocol for informative visualization of enriched gene ontology terms. Bio-Protocol **9**

Book AJ, Gladman NP, Lee SS, Scalf M, Smith LM, Vierstra RD (2010) Affinity purification of the Arabidopsis 26 S proteasome reveals a diverse array of plant proteolytic complexes. J Biol Chem **285**: 25554–25569

Chen XL, Xie X, Wu L, Liu C, Zeng L, Zhou X, Luo F, Wang GL, Liu W (2018) Proteomic analysis of ubiquitinated proteins in rice (*Oryza sativa*) after treatment with pathogen-associated molecular pattern (PAMP) elicitors. Front Plant Sci **9**: 1064

Chen Y, Li F, Tian L, Huang M, Deng R, Li X, Chen W, Wu P, Li M, Jiang H (2017) The phenylalanine ammonia lyase gene LJPAL1 is involved in plant defense responses to pathogens and plays diverse roles in *Lotus japonicus*-rhizobium symbioses. Mol Plant Microb Interact **30**: 739–753

Cheng YT, Li X (2012) Ubiquitination in NB-LRR-mediated immunity. Curr Opin Plant Biol **15**: 392–399

Cheng YT, Li YZ, Huang SA, Huang Y, Dong XN, Zhang YL, Li X (2011) Stability of plant immune-receptor resistance proteins is controlled by SKP1-CULLIN1-F-box (SCF)-mediated protein degradation. Proc Natl Acad Sci U S A **108**: 14694–14699

Cheng Z, Li JF, Niu Y, Zhang XC, Woody OZ, Xiong Y, Djonovic S, Millet Y, Bush J, McConkey BJ, et al. (2015) Pathogen-secreted proteases activate a novel plant immune pathway. Nature **521**: 213–216

Clay NK, Adio AM, Denoux C, Jander G, Ausubel FM (2009) Glucosinolate metabolites required for an Arabidopsis innate immune response. Science **323**: 95–101

Collins NC, Thordal-Christensen H, Lipka V, Bau S, Kombrink E, Qiu JL, Huckelhoven R, Stein M, Freialdenhoven A, Somerville SC, et al. (2003) SNARE-protein-mediated disease resistance at the plant cell wall. Nature **425**: 973–977

Couto D, Zipfel C (2016) Regulation of pattern recognition receptor signalling in plants. Nat Rev Immunol **16**: 537–552

Cui H, Tsuda K, Parker JE (2015) Effector-triggered immunity: from pathogen perception to robust defense. Annu Rev Plant Biol **66**: 487–511

Dielen AS, Badaoui S, Candresse T, German-Retana S (2010) The ubiquitin/26S proteasome system in plant–pathogen interactions: a never-ending hide-and-seek game. Mol Plant Pathol **11**: 293–308

Eng JK, McCormack AL, Yates JR (1994) An approach to correlate tandem mass spectral data of peptides with amino acid sequences in a protein database. J Am Soc Mass Spectrom **5**: 976–989

Eschen-Lippold L, Bethke G, Palm-Forster MA, Pecher P, Bauer N, Glazebrook J, Scheel D, Lee J (2012) MPK11—a fourth elicitor-responsive mitogen-activated protein kinase in *Arabidopsis thaliana*. Plant Signal Behav **7**: 1203–1205

Ewan R, Pangestuti R, Thornber S, Craig A, Carr C, O'Donnell L, Zhang C, Sadanandom A (2011) Deubiquitinating enzymes AtUBP12 and AtUBP13 and their tobacco homologue NtUBP12 are negative regulators of plant immunity. New Phytol **191**: 92–106

Finley D (2009) Recognition and processing of ubiquitin-protein conjugates by the proteasome. Annu Rev Biochem **78**: 477–513

Fuchs R, Kopischke M, Klapprodt C, Hause G, Meyer AJ, Schwarzlander M, Fricker MD, Lipka V (2016) Immobilized subpopulations of leaf epidermal mitochondria mediate PENETRATION2-dependent pathogen entry control in Arabidopsis. Plant Cell **28**: 130–145

Furlan G, Nakagami H, Eschen-Lippold L, Jiang X, Majovsky P, Kowarschik K, Hoehenwarter W, Lee J, Trujillo M (2017) Changes in PUB22 ubiquitination modes triggered by MITOGEN-ACTIVATED PROTEIN KINASE3 dampen the immune response. Plant Cell **29**: 726–745

Furniss JJ, Grey H, Wang ZS, Nomoto M, Jackson L, Tada Y, Spoel SH (2018) Proteasome-associated HECT-type ubiquitin ligase activity is required for plant immunity. PLoS Pathog **14**: e1007447

Goritschnig S, Zhang YL, Li X (2007) The ubiquitin pathway is required for innate immunity in Arabidopsis. Plant J **49**: 540–551

Gou M, Shi Z, Zhu Y, Bao Z, Wang G, Hua J (2012) The F-box protein CPR1/CPR30 negatively regulates R protein SNC1 accumulation. Plant J **69**: 411–420

Gou M, Su N, Zheng J, Huai J, Wu G, Zhao J, He J, Tang D, Yang S, Wang GJTPJ (2009) An F-box gene, CPR30, functions as a negative regulator of the defense response in Arabidopsis. Plant J **60**: 757–770

Gu Y, Innes RW (2011) The KEEP ON GOING protein of Arabidopsis recruits the ENHANCED DISEASE RESISTANCE1 protein to trans-Golgi network/early endosome vesicles. Plant Physiol **155**: 1827–1838

Gu Y, Zavaliev R, Dong X (2017) Membrane trafficking in plant immunity. Mol Plant **10**: 1026–1034

Guerra DD, Callis J (2012) Ubiquitin on the move: the ubiquitin modification system plays diverse roles in the regulation of endoplasmic reticulum- and plasma membrane-localized proteins. Plant Physiol **160**: 56–64

Heidrich K, Wirthmueller L, Tasset C, Pouzet C, Deslandes L, Parker JE (2011) Arabidopsis EDS1 connects pathogen effector recognition to cell compartment-specific immune responses. Science **334**: 1401–1404

Hjerpe R, Aillet F, Lopitz-Otsoa F, Lang V, England P, Rodriguez MS (2009) Efficient protection and isolation of ubiquitylated proteins using tandem ubiquitin-binding entities. EMBO Rep **10**: 1250–1258

Hou S, Wang X, Chen D, Yang X, Wang M, Turra D, Di Pietro A, Zhang W (2014) The secreted peptide PIP1 amplifies immunity through receptor-like kinase 7. PLoS Pathog **10**: e1004331

Hou X, Gao Y (2017) Investigation on the interaction of *Pseudomonas syringae* effector AvrPto with AtRabE1d GTPase. Protein Peptide Lett **24**: 661–667

Hu HB, Sun SC (2016) Ubiquitin signaling in immune responses. Cell Res **26**: 457–483

Hua Z, Vierstra RD (2011) The cullin-RING ubiquitin-protein ligases. Annu Rev Plant Biol **62**: 299–334

Huang da W, Sherman BT, Lempicki RA (2009) Systematic and integrative analysis of large gene lists using DAVID bioinformatics resources. Nat Protoc **4**: 44–57

Huang J, Gu M, Lai Z, Fan B, Shi K, Zhou YH, Yu JQ, Chen Z (2010) Functional analysis of the Arabidopsis PAL gene family in plant growth, development, and response to environmental stress. Plant Physiol **153**: 1526–1538

Huang S, Chen X, Zhong X, Li M, Ao K, Huang J, Li X (2016) Plant TRAF proteins regulate NLR immune receptor turnover. Cell Host Microbe **20**: 271

Isono E, Nagel MK (2014) Deubiquitylating enzymes and their emerging role in plant biology. Front Plant Sci **5**: 56

Iwai K, Tokunaga F (2009) Linear polyubiquitination: a new regulator of NF-kappaB activation. EMBO Rep **10**: 706–713

Jacobs AK, Lipka V, Burton RA, Panstruga R, Strizhov N, Schulze-Lefert P, Fincher GB (2003) An Arabidopsis callose synthase, GSL5, is required for wound and papillary callose formation. Plant Cell **15**: 2503–2513

Johnson A, Vert G (2016) Unraveling K63 polyubiquitination networks by sensor-based proteomics. Plant Physiol **171**: 1808–1820

Kim DY, Scalf M, Smith LM, Vierstra RD (2013) Advanced proteomic analyses yield a deep catalog of ubiquitylation targets in Arabidopsis. Plant Cell **25**: 1523–1540

Kim SJ, Kim MR, Bedgar DL, Moinuddin SG, Cardenas CL, Davin LB, Kang C, Lewis NG (2004) Functional reclassification of the putative cinnamyl alcohol dehydrogenase multigene family in Arabidopsis. Proc Natl Acad Sci U S A **101**: 1455–1460

Downloaded from https://academic.oup.com/plphys/article/185/4/1943/6122724 by guest on 30 April 2021

Kleinboelting N, Huep G, Kloetgen A, Viehoever P, Weisshaar B (2012) GABI-Kat SimpleSearch: new features of the *Arabidopsis thaliana* T-DNA mutant database. Nucleic Acids Res **40**: D1211–D1215

Komander D, Rape M (2012) The ubiquitin code. Annu Rev Biochem **81**: 203–229

Lachaud C, Prigent E, Thuleau P, Grat S, Da Silva D, Brière C, Mazars C, Cotelle V (2013) 14-3-3-regulated Ca^{2+}-dependent protein kinase CPK3 is required for sphingolipid-induced cell death in Arabidopsis. Cell Death Differ **20**: 209–217

Lapin D, Bhandari DD, Parker JE (2020) Origins and immunity networking functions of EDS1 family proteins. Annu Rev Phytopathol **58**: 253–276

Le MH, Cao Y, Zhang XC, Stacey G (2014) LIK1, a CERK1-interacting kinase, regulates plant immune responses in Arabidopsis. PLoS ONE **9**: e102245

Lee B-J, Kwon SJ, Kim S-K, Kim K-J, Park C-J, Kim Y-J, Park OK, Paek K-H (2006) Functional study of hot pepper 26S proteasome subunit RPN7 induced by Tobacco mosaic virus from nuclear proteome analysis. Biochem Biophys Res Commun **351**: 405–411

Li L, Habring A, Wang K, Weigel D (2020) Atypical resistance protein RPW8/HR triggers oligomerization of the NLR immune receptor RPP7 and autoimmunity. Cell Host Microbe **27**: 405–417.e406

Li Y, Kabbage M, Liu W, Dickman MB (2016) Aspartyl protease-mediated cleavage of BAG6 is necessary for autophagy and fungal resistance in plants. Plant Cell **28**: 233–247

Liang X, Ding P, Lian K, Wang J, Ma M, Li L, Li L, Li M, Zhang X, Chen S, et al. (2016) Arabidopsis heterotrimeric G proteins regulate immunity by directly coupling to the FLS2 receptor. Elife **5**: e13568

Liao D, Cao Y, Sun X, Espinoza C, Nguyen CT, Liang Y, Stacey G (2017) Arabidopsis E3 ubiquitin ligase PLANT U-BOX13 (PUB13) regulates chitin receptor LYSIN MOTIF RECEPTOR KINASE5 (LYK5) protein abundance. New Phytol **214**: 1646–1656

Liebrand TW, van den Burg HA, Joosten MH (2014) Two for all: receptor-associated kinases SOBIR1 and BAK1. Trends Plant Sci **19**: 123–132

Liu J, Ding P, Sun T, Nitta Y, Dong O, Huang X, Yang W, Li X, Botella JR, Zhang Y (2013) Heterotrimeric G proteins serve as a converging point in plant defense signaling activated by multiple receptor-like kinases. Plant Physiol **161**: 2146–2158

Liu JK, Li HJ, Miao M, Tang XF, Giovannoni J, Xiao FM, Liu YS (2012) The tomato UV-damaged DNA-binding protein-1 (DDB1) is implicated in pathogenesis-related (PR) gene expression and resistance to *Agrobacterium tumefaciens*. Mol Plant Pathol **13**: 123–134

Lu D, Lin W, Gao X, Wu S, Cheng C, Avila J, Heese A, Devarenne TP, He P, Shan L (2011) Direct ubiquitination of pattern recognition receptor FLS2 attenuates plant innate immunity. Science **332**: 1439–1442

Ma X, Claus LAN, Leslie ME, Tao K, Wu Z, Liu J, Yu X, Li B, Zhou J, Savatin DV, et al. (2020) Ligand-induced monoubiquitination of BIK1 regulates plant immunity. Nature **581**: 199–203

Maor R, Jones A, Nuhse TS, Studholme DJ, Peck SC, Shirasu K (2007) Multidimensional protein identification technology (MudPIT) analysis of ubiquitinated proteins in plants. Mol Cell Proteomics **6**: 601–610

Marino D, Peeters N, Rivas S (2012) Ubiquitination during plant immune signaling. Plant Physiol **160**: 15–27

Marshall RS, Li F, Gemperline DC, Book AJ, Vierstra RD (2015) Autophagic degradation of the 26S proteasome is mediated by the dual ATG8/ubiquitin receptor RPN10 in Arabidopsis. Mol Cell **58**: 1053–1066

Marshall RS, Vierstra RD (2018) Autophagy: the master of bulk and selective recycling. Annu Rev Plant Biol **69**: 173–208

Meng X, Zhang S (2013) MAPK cascades in plant disease resistance signaling. Annu Rev Phytopathol **51**: 245–266

Meyer D, Pajonk S, Micali C, O'Connell R, Schulze-Lefert PJTPJ (2009) Extracellular transport and integration of plant secretory proteins into pathogen-induced cell wall compartments. Plant J **57**: 986–999

Miao Y, Zentgraf U (2010) A HECT E3 ubiquitin ligase negatively regulates Arabidopsis leaf senescence through degradation of the transcription factor WRKY53. Plant J **63**: 179–188

Monaghan J, Li X (2010) The HEAT repeat protein ILITYHIA is required for plant immunity. Plant Cell Physiol **51**: 742–753

Monaghan J, Xu F, Gao M, Zhao Q, Palma K, Long C, Chen S, Zhang Y, Li X (2009) Two Prp19-like U-box proteins in the MOS4-associated complex play redundant roles in plant innate immunity. PLoS Pathog **51**: 742–753

Mondragon-Palomino M, Stam R, John-Arputharaj A, Dresselhaus T (2017) Diversification of defensins and NLRs in Arabidopsis species by different evolutionary mechanisms. BMC Evol Biol **17**: 255

Mural RV, Liu Y, Rosebrock TR, Brady JJ, Hamera S, Connor RA, Martin GB, Zeng L (2013) The tomato Fni3 lysine-63-specific ubiquitin-conjugating enzyme and suv ubiquitin E2 variant positively regulate plant immunity. Plant Cell **25**: 3615–3631

Murata S, Yashiroda H, Tanaka K (2009) Molecular mechanisms of proteasome assembly. Nat Rev Mol Cell Biol **10**: 104–115

Nakashima A, Chen L, Thao NP, Fujiwara M, Wong HL, Kuwano M, Umemura K, Shirasu K, Kawasaki T, Shimamoto K (2008) RACK1 functions in rice innate immunity by interacting with the Rac1 immune complex. Plant Cell **20**: 2265–2279

Nicaise V, Joe A, Jeong B, Korneli C, Boutrot F, Wested I, Staiger D, Alfano J, Zipfel C (2013) Pseudomonas HopU1 affects interaction of plant immune receptor mRNAs to the RNA-binding protein GRP7. EMBO J **32**: 701–712

Okumoto K, Misono S, Miyata N, Matsumoto Y, Mukai S, Fujiki Y (2011) Cysteine ubiquitination of PTS1 receptor Pex5p regulates Pex5p recycling. Traffic **12**: 1067–1083

Ordureau A, Paulo JA, Zhang J, An H, Swatek KN, Cannon JR, Wan Q, Komander D, Harper JW (2020) Global landscape and dynamics of Parkin and USP30-dependent ubiquitylomes in iNeurons during mitophagic signaling. Mol Cell **77**: 1124–1142.e1110

Paez Valencia J, Goodman K, Otegui MS (2016) Endocytosis and endosomal trafficking in plants. Annu Rev Plant Biol **67**: 309–335

Palm D, Streit D, Shanmugam T, Weis BL, Ruprecht M, Simm S, Schleiff E (2019) Plant-specific ribosome biogenesis factors in *Arabidopsis thaliana* with essential function in rRNA processing. Nucleic Acids Res **47**: 1880–1895

Parker JE, Holub EB, Frost LN, Falk A, Gunn ND, Daniels MJ (1996) Characterization of eds1, a mutation in Arabidopsis suppressing resistance to *Peronospora parasitica* specified by several different RPP genes. Plant Cell **8**: 2033–2046

Pastorczyk M, Bednarek P (2016) The function of glucosinolates and related metabolites in plant innate immunity. In Advances in Botanical Research, **80**, Elsevier, pp. 171–198

Pecher P, Eschen-Lippold L, Herklotz S, Kuhle K, Naumann K, Bethke G, Uhrig J, Weyhe M, Scheel D, Lee J (2014) The *Arabidopsis thaliana* mitogen-activated protein kinases MPK 3 and MPK 6 target a subclass of 'VQ-motif'-containing proteins to regulate immune responses. New Phytol **203**: 592–606

Peng J, Schwartz D, Elias JE, Thoreen CC, Cheng D, Marsischky G, Roelofs J, Finley D, Gygi SP (2003) A proteomics approach to understanding protein ubiquitination. Nat Biotechnol **21**: 921–926

Perraki A, Gronnier J, Gouguet P, Boudsocq M, Deroubaix A-F, Simon V, German-Retana S, Zipfel C, Bayer E, Mongrand S (2017) The plant calcium-dependent protein kinase CPK3 phosphorylates REM1.3 to restrict viral infection. BioRxiv, 205765

Pitorre D, Llauro C, Jobet E, Guilleminot J, Brizard J-P, Delseny M, Lasserre E (2010) RLK7, a leucine-rich repeat receptor-like kinase, is required for proper germination speed and tolerance to oxidative stress in *Arabidopsis thaliana*. Planta **232**: 1339–1353

Qin L, Zhou Z, Li Q, Zhai C, Liu L, Quilichini TD, Gao P, Kessler SA, Jaillais Y, Datla R, et al. (2020) Specific recruitment of phosphoinositide species to the plant–pathogen interfacial membrane

Downloaded from https://academic.oup.com/plphys/article/185/4/1943/6122724 by guest on 30 April 2021

underlies Arabidopsis susceptibility to fungal infection. Plant Cell **32**: 1665–1688

Raasi S, Orlov I, Fleming KG, Pickart CM (2004) Binding of polyubiquitin chains to ubiquitin-associated (UBA) domains of HHR23A. J Mol Biol **341**: 1367–1379

Rayapuram N, Bigeard J, Alhoraibi H, Bonhomme L, Hesse AM, Vinh J, Hirt H, Pflieger D (2018) Quantitative phosphoproteomic analysis reveals shared and specific targets of Arabidopsis mitogen-activated protein kinases (MAPKs) MPK3, MPK4, and MPK6. Mol Cell Proteomics **17**: 61–80

Revers F, Guiraud T, Houvenaghel M-C, Mauduit T, Le Gall O, Candresse T (2003) Multiple resistance phenotypes to Lettuce mosaic virus among *Arabidopsis thaliana* accessions. Mol Plant Microb Interact **16**: 608–616

Reyes FC, Buono R, Otegui MS (2011) Plant endosomal trafficking pathways. Curr Opin Plant Biol **14**: 666–673

Rodrigues O, Reshetnyak G, Grondin A, Saijo Y, Leonhardt N, Maurel C, Verdoucq L (2017) Aquaporins facilitate hydrogen peroxide entry into guard cells to mediate ABA- and pathogen-triggered stomatal closure. Proc Natl Acad Sci U S A **114**: 9200–9205

Romero-Barrios N, Vert G (2018) Proteasome-independent functions of lysine-63 polyubiquitination in plants. New Phytol **217**: 995–1011

Saracco SA, Hansson M, Scalf M, Walker JM, Smith LM, Vierstra RD (2009) Tandem affinity purification and mass spectrometric analysis of ubiquitylated proteins in Arabidopsis. Plant J **59**: 344–358

Shannon P, Markiel A, Ozier O, Baliga NS, Wang JT, Ramage D, Amin N, Schwikowski B, Ideker T (2003). Cytoscape: a software environment for integrated models of biomolecular interaction networks. Genome Res **13**: 2498–2504

Shimizu Y, Okuda-Shimizu Y, Hendershot LM (2010) Ubiquitylation of an ERAD substrate occurs on multiple types of amino acids. Mol Cell **40**: 917–926

Skubacz A, Daszkowska-Golec A, Szarejko I (2016) The role and regulation of ABI5 (ABA-insensitive 5) in plant development, abiotic stress responses and phytohormone crosstalk. Front Plant Sci **7**:1884

Smalle J, Vierstra RD (2004) The ubiquitin 26S proteasome proteolytic pathway. Annu Rev Plant Biol **55**: 555–590

Speth EB, Imboden L, Hauck P, He SY (2009) Subcellular localization and functional analysis of the Arabidopsis GTPase RabE. Plant Physiol **149**: 1824–1837

Spoel SH, Dong X (2012) How do plants achieve immunity? Defence without specialized immune cells. Nat Rev Immunol **12**: 89–100

Stegmann M, Anderson RG, Ichimura K, Pecenkova T, Reuter P, Zarsky V, McDowell JM, Shirasu K, Trujillo M (2012) The ubiquitin ligase PUB22 targets a subunit of the exocyst complex required for PAMP-triggered responses in Arabidopsis. Plant Cell **24**: 4703–4716

Stringlis IA, Yu K, Feussner K, de Jonge R, Van Bentum S, Van Verk MC, Berendsen RL, Bakker PA, Feussner I, Pieterse CM (2018) MYB72-dependent coumarin exudation shapes root microbiome assembly to promote plant health. Proc Natl Acad Sci U S A **115**: E5213–E5222

Su J, Xu J, Zhang S (2015) RACK1, scaffolding a heterotrimeric G protein and a MAPK cascade. Trends Plant Sci **20**: 405–407

Su J, Yang L, Zhu Q, Wu H, He Y, Liu Y, Xu J, Jiang D, Zhang S (2018) Active photosynthetic inhibition mediated by MPK3/MPK6 is critical to effector-triggered immunity. PLoS Biol **16**: e2004122

Szklarczyk D, Franceschini A, Wyder S, Forslund K, Heller D, Huerta-Cepas J, Simonovic M, Roth A, Santos A, Tsafou KP, et al. (2015) STRING v10: protein–protein interaction networks, integrated over the tree of life. Nucleic Acids Res **43**: D447–D452

Tan X, Meyers BC, Kozik A, West MA, Morgante M, St Clair DA, Bent AF, Michelmore RW (2007) Global expression analysis of nucleotide binding site-leucine rich repeat-encoding and related genes in Arabidopsis. BMC Plant Biol **7**: 56

Tarutani Y, Morimoto T, Sasaki A, Yasuda M, Nakashita H, Yoshida S, Yamaguchi I, Suzuki Y (2004) Molecular characterization of two highly homologous receptor-like kinase genes, RLK902 and RKL1, in *Arabidopsis thaliana*. Biosci Biotechnol Biochem **68**: 1935–1941

Thordal-Christensen H (2003) Fresh insights into processes of non-host resistance. Curr Opin Plant Biol **6**: 351–357

Tronchet M, Balague C, Kroj T, Jouanin L, Roby D (2010) Cinnamyl alcohol dehydrogenases-C and D, key enzymes in lignin biosynthesis, play an essential role in disease resistance in Arabidopsis. Mol Plant Pathol **11**: 83–92

Trujillo M, Shirasu K (2010) Ubiquitination in plant immunity. Curr Opin Plant Biol **13**: 402–408

Udeshi ND, Svinkina T, Mertins P, Kuhn E, Mani DR, Qiao JW, Carr SA (2013) Refined preparation and use of anti-diglycine remnant (K-epsilon-GG) antibody enables routine quantification of 10,000s of ubiquitination sites in single proteomics experiments. Mol Cell Proteomics **12**: 825–831

Urano D, Chen JG, Botella JR, Jones AM (2013) Heterotrimeric G protein signalling in the plant kingdom. Open Biol **3**: 120186

Üstün S, Sheikh A, Gimenez-Ibanez S, Jones A, Ntoukakis V, Börnke F (2016) The proteasome acts as a hub for plant immunity and is targeted by Pseudomonas type III effectors. Plant Physiol **172**: 1941–1958

van Nocker S, Walker JM, Vierstra RD (1996) The *Arabidopsis thaliana* UBC7/13/14 genes encode a family of multiubiquitin chain-forming E2 enzymes. J Biol Chem **271**: 12150–12158

Vierstra RD (2009) The ubiquitin-26S proteasome system at the nexus of plant biology. Nat Rev Mol Cell Biol **10**: 385–397

Wang J, Grubb LE, Wang J, Liang X, Li L, Gao C, Ma M, Feng F, Li M, Li L, et al. (2018) A regulatory module controlling homeostasis of a plant immune kinase. Mol Cell **69**: 493–504.e6

Wang L, Wen R, Wang J, Xiang D, Wang Q, Zang Y, Wang Z, Huang S, Li X, Datla R, et al. (2019) Arabidopsis UBC 13 differentially regulates two programmed cell death pathways in responses to pathogen and low-temperature stress. New Phytol **221**: 919–934

Wawrzynska A, Rodibaugh NL, Innes RW (2010) Synergistic activation of defense responses in Arabidopsis by simultaneous loss of the GSL5 callose synthase and the EDR1 protein kinase. Mol Plant Microbe Interact **23**: 578–584

Wen R, Torres-Acosta JA, Pastushok L, Lai X, Pelzer L, Wang H, Xiao W (2008) Arabidopsis UEV1D promotes lysine-63-linked polyubiquitination and is involved in DNA damage response. Plant Cell **20**: 213–227

Yao C, Wu Y, Nie H, Tang D (2012) RPN1a, a 26S proteasome subunit, is required for innate immunity in Arabidopsis. Plant J **71**: 1015–1028

Yin Z, Popelka H, Lei Y, Yang Y, Klionsky DJ (2020) The roles of ubiquitin in mediating autophagy. Cells **9**: 2025

Yu X, Feng B, He P, Shan L (2017) From chaos to harmony: responses and signaling upon microbial pattern recognition. Annu Rev Phytopathol **55**: 109–137

Zamioudis C, Hanson J, Pieterse CM (2014) β-Glucosidase BGLU 42 is a MYB 72-dependent key regulator of rhizobacteria-induced systemic resistance and modulates iron deficiency responses in Arabidopsis roots. New Phytol **204**: 368–379

Zhao J, Zhou H, Zhang M, Gao Y, Li L, Gao Y, Li M, Yang Y, Guo Y, Li X (2016) Ubiquitin-specific protease 24 negatively regulates abscisic acid signalling in *Arabidopsis thaliana*. Plant Cell Environ **39**: 427–440

Downloaded from https://academic.oup.com/plphys/article/185/4/1943/6122724 by guest on 30 April 2021

Zhao Y, Wu G, Shi H, Tang D (2019) RECEPTOR-LIKE KINASE 902 associates with and phosphorylates BRASSINOSTEROID-SIGNALING KINASE1 to regulate plant immunity. Mol Plant **12**: 59–70

Zhou B, Zeng L (2017) Conventional and unconventional ubiquitination in plant immunity. Mol Plant Pathol **18**: 1313–1330

Zhou J-M, Zhang Y (2020) Plant immunity: danger perception and signaling. Cell **181**: 978–989

Zhou J, He P, Shan L (2014) Ubiquitination of plant immune receptors. Methods Mol Biol **1209**: 219–231

Zhou J, Liu D, Wang P, Ma X, Lin W, Chen S, Mishev K, Lu D, Kumar R, Vanhoutte I, et al. (2018) Regulation of Arabidopsis brassinosteroid receptor BRI1 endocytosis and degradation by plant U-box PUB12/PUB13-mediated ubiquitination. Proc Natl Acad Sci U S A **115**: E1906–E1915

Zhou J, Lu D, Xu G, Finlayson SA, He P, Shan L (2015) The dominant negative ARM domain uncovers multiple functions of PUB13 in Arabidopsis immunity, flowering, and senescence. J Exp Bot **66**: 3353–3366

Downloaded from https://academic.oup.com/plphys/article/185/4/1943/6122724 by guest on 30 April 2021